© 2014. Published by The Company of Biologists Ltd | Development (2014) 141, 3165-3176 doi:10.1242/dev.109181

RESEARCH ARTICLE

Auxin represses stomatal development in dark-grown seedlings via Aux/IAA proteins

Martin Balcerowicz, Aashish Ranjan*, Laura Rupprecht, Gabriele Fiene‡ and Ute Hoecker§

ABSTRACT

Stomatal development is tightly regulated through internal and external factors that are integrated by a complex signalling network. Light represents an external factor that strongly promotes stomata formation. Here, we show that auxin-resistant *aux*/*iaa* mutants, e.g. *axr3-1*, exhibit a de-repression of stomata differentiation in dark-grown seedlings. The higher stomatal index in dark-grown *axr3-1* mutants when compared with the wild type is due to increased cell division in the stomatal lineage. Excessive stomata in dark-grown seedlings were also observed in mutants defective in auxin biosynthesis or auxin perception and in seedlings treated with the polar auxin transport inhibitor NPA. Consistent with these findings, exogenous auxin repressed stomata formation in light-grown seedlings. Taken together, these results indicate that auxin is a negative regulator of stomatal development in dark-grown seedlings. Epistasis analysis revealed that *axr3-1* acts genetically upstream of the bHLH transcription factors SPCH, MUTE and FAMA, as well as the YDA MAP kinase cascade, but in parallel with the repressor of photomorphogenesis COP1 and the receptor-like protein TMM. The effect of exogenous auxin required the ER family of leucine-rich repeat receptor-like kinases, suggesting that auxin acts at least in part through the ER family. Expression of *axr3-1* in the stomatal lineage was insufficient to alter the stomatal index, implying that cell-cell communication is necessary to mediate the effect of auxin. In summary, our results show that auxin signalling contributes to the suppression of stomatal differentiation observed in dark-grown seedlings.

KEY WORDS: Stomatal development, Auxin, Aux/IAA proteins, Photomorphogenesis, *Arabidopsis*

INTRODUCTION

Stomata are epidermal pores that are crucial for plant survival, as they balance gas exchange and transpiration, thereby strongly affecting photosynthetic performance. Hence, not only stomatal opening but also stomatal development is tightly regulated. In *Arabidopsis*, stomata are produced by a subset of protodermal cells. A protodermal cell can either divide symmetrically to form pavement cells or it becomes a meristemoid mother cell (MMC) that divides asymmetrically to enter the stomatal lineage. This asymmetric division gives rise to a larger stomatal lineage ground cell (SLGC) and a smaller meristemoid, which retains self-renewing capability. The meristemoid can divide asymmetrically twice more before it differentiates into a guard mother cell (GMC). The GMC undergoes one symmetric division, producing two guard cells that form a stoma. The surrounding SLGCs can either differentiate into pavement cells or can undergo additional asymmetric divisions, thereby giving rise to satellite meristemoids. These divisions are referred to as spacing divisions, as the new meristemoid is always formed away from the existing stoma. As a consequence, two stomata are normally separated by at least one pavement cell ('one-cell-spacing rule') (Pillitteri and Torii, 2012; Wengier and Bergmann, 2012).

Three bHLH transcription factors, SPEECHLESS (SPCH), MUTE and FAMA, control consecutive steps of stomatal development. SPCH promotes entry and amplifying divisions in the stomatal lineage (MacAlister et al., 2007; Pillitteri et al., 2007). MUTE is required for the termination of amplifying divisions and the cell-state transition from the meristemoid to the GMC (Pillitteri et al., 2007). FAMA restricts symmetric division of the GMC to one round and promotes the transition to guard cells (Ohashi-Ito and Bergmann, 2006). Two additional bHLH proteins, SCREAM (SCRM)/INDUCER OF CBF1 (ICE1) and SCRM2, with largely redundant functions, act in concert with the aforementioned bHLH proteins to promote all steps of stomatal development (Kanaoka et al., 2008).

Upstream of these bHLH transcription factors, a MAP kinase cascade, comprising the MAP kinase kinase kinase YDA, the MAP kinase kinases MKK4 and MKK5 and the MAP kinases MPK4, MPK5, MPK7 and MPK9, suppresses stomatal development (Bergmann et al., 2004; Lampard et al., 2008, 2009; Wang et al., 2007). Additional negative regulators act upstream of this cascade: leucine-rich repeat (LRR) receptor-like kinases of the ERECTA (ER) family (ERf), consisting of ER, ERECTA-LIKE1 (ERL1) and ERL2, control stomatal patterning and differentiation (Shpak et al., 2005). Activity of the ERf is modulated by the LRR receptor-like protein TOO MANY MOUTHS (TMM). In cotyledons and leaves, it restricts stomata differentiation and guides spacing divisions in concert with the ERf, but in hypocotyls and stems, it promotes stomatal development and thereby antagonises ERf function (Bhave et al., 2009; Nadeau and Sack, 2002; Shpak et al., 2005; Yang and Sack, 1995). Activity of the TMM-ERf module is controlled by cysteine-rich peptide ligands of the EPIDERMAL PATTERNING FACTOR-LIKE (EPFL) family (Lee et al., 2012; Rychel et al., 2010).

Light strongly promotes stomatal development, as stomata are found at very low numbers in the cotyledon epidermis of dark-grown seedlings. The photoreceptors cryptochromes, phytochrome A (phyA) and phyB promote the differentiation of stomata in the light. phyB has been recently shown to act systemically in stomata cell fate determination, indicating that phyB action in mature leaves modulates stomatal differentiation in young leaves (Casson and Hetherington, 2014). Downstream of these photoreceptors, a repressor of light signalling, consisting of CONSTITUTIVELY PHOTOMORPHOGENIC1 (COP1) and SUPPRESSOR OF

Botanical Institute and Cluster of Excellence on Plant Sciences (CEPLAS), University of Cologne, BioCenter, Zuelpicher Str. 47b, 50674 Cologne, Germany. *Present address: Department of Plant Biology, UC Davis, One Shields Avenue, Davis, CA 95616, USA. ‡Present address: Australian Centre for Plant Functional Genomics, University of Adelaide, Waite Campus, Hartley Grove Urrbrae, SA 5064, Australia.

§Author for correspondence (hoeckeru@uni-koeln.de)

Received 19 February 2014; Accepted 29 June 2014

Development (2014) 141, 3165-3176 doi:10.1242/dev.109181

PHYTOCHROME A-105 (SPA) proteins, acts to inhibit stomatal development in darkness (Kang et al., 2009). In addition, phyB and PHYTOCHROME INTERACTING FACTOR4 (PIF4) regulate stomata formation in true leaves in response to high light intensities (Boccalandro et al., 2009; Casson et al., 2009).

Phytohormones also control stomatal development. Brassinosteroids (BRs) regulate the phosphorylation state of SPCH and components of the YDA MAPK cascade and thereby affect stomatal development (Gudesblat et al., 2012; Khan et al., 2013; Kim et al., 2012). It has been recently shown that polar auxin transport is crucial for maintaining the one-cell-spacing rule in stomatal patterning. High auxin activity has been observed during unequal cell divisions, whereas a decrease in auxin activity promotes GMC fate and its subsequent equal division into two guard cells (Le et al., 2014).

Auxin is perceived by two sets of receptors: the plasma membrane-localised AUXIN BINDING PROTEIN1 (ABP1) and the nuclear TRANSPORT INHIBITOR RESPONSE1 (TIR1)/AUXIN-BINDING F-BOX (AFB) proteins (Hayashi, 2012). TIR1/AFB proteins control the abundance of AUXIN/INDOLE-3-ACETIC ACID (AUX/IAA) repressors. At low auxin concentrations, AUX/IAA proteins inhibit the transcriptional regulatory function of AUXIN RESPONSE FACTORS (ARFs) (Tiwari et al., 2001; Ulmasov et al., 1999). Auxin promotes the formation of a TIR1/AFB-AUX/IAA co-receptor complex, leading to ubiquitylation and subsequent degradation of AUX/IAA proteins, which results in de-repression of ARFs (Dharmasiri et al., 2005a,b; Gray et al., 2001; Kepinski and Leyser, 2005; Tan et al., 2007).

Mutant AUX/IAA proteins that fail to interact with the auxin receptor are not degraded in the presence of auxin and, therefore, lead to auxin insensitivity (Reed, 2001). Such gain-of-function mutations in the *AUX*/*IAA* genes *SHORT HYPOCOTYL2* (*SHY2*)/*IAA3*, *AUXIN RESISTANT2* (*AXR2*)/*IAA7* and *AXR3*/*IAA17* result in a constitutive photomorphogenesis phenotype characterised by a short hypocotyl and open cotyledons in dark-grown seedlings (Leyser et al., 1996; Reed et al., 1998; Timpte et al., 1994). Here, we report that these mutants are defective in the suppression of stomatal development in darkness and that *AXR3* acts genetically upstream of the YDA MAP kinase cascade to regulate stomata formation in response to light and auxin signals.

RESULTS

Gain-of-function *aux*/*iaa* mutants fail to suppress stomata differentiation in dark-grown seedlings

The gain-of-function *aux*/*iaa* mutants *axr2-1*, *axr3-1* and *shy2-2* display a constitutive photomorphogenesis phenotype similar to, although less pronounced than, the *cop1-4* mutant, with short hypocotyls and partially opened cotyledons when grown in darkness (Leyser et al., 1996; Reed et al., 1998; Timpte et al., 1994) (Fig. 1A). We investigated whether the *aux*/*iaa* mutants also exhibit a defect in the suppression of stomatal development in dark-grown seedlings. Indeed, the stomatal index (SI), i.e. the proportion of stomata among all epidermal cells, was increased in dark-grown *axr2-1*, *axr3-1* and *shy2-2* mutant seedlings when compared with the wild type (Fig. 1B,C; supplementary material Fig. S1). Again, this aspect of the *aux/iaa* mutant phenotype was similar to, but less dramatic, than that of the *cop1-4* mutant (Fig. 1B,C). The proportion of stomatal precursors, i.e. meristemoids and GMCs, was not changed or only mildly reduced in the three *aux*/*iaa* mutants. In hypocotyls of dark-grown *aux*/*iaa* mutant seedlings, stomata differentiation was also enhanced when compared with the wild type (Fig. 1F). The *axr2-1 axr3-1* double mutant displayed no additional increase in stomata formation when compared with the single mutants (supplementary material Fig. S2). Clustered stomata were not observed in any of the *axr* single or double mutants.

The stomata-overproducing phenotype of the *aux*/*iaa* mutants was specific to dark-grown seedlings. No major changes in the percentage of stomata and stomatal precursors were observed in cotyledons of light-grown seedlings or in true leaves of adult plants except for a slight reduction of the SI in the cotyledons of *axr3-1*, which, however, was not observed in *axr2-1* (Fig. 1D,E; supplementary material Fig. S1).

The *axr3-1* mutation causes a post-embryonic increase in the division of stomatal lineage cells

Cotyledons of dark-grown seedlings were examined over a time course from 2 to 10 days post germination (dpg). Virtually no mature stomata were observed in the cotyledon epidermis of 2-day-old wild-type, *axr2-1* and *axr3-1* mutant seedlings; the first stomata appeared between 3 and 4 dpg and excessive stomata developed in *axr2-1* and *axr3-1* in the following days (Fig. 2A). Hence, stomata in *aux/iaa* mutants do not form prematurely but post-embryonically, similar to the wild type.

We subsequently investigated how the increased SI in dark-grown *axr3-1* reflects the total, absolute number of stomata and pavement cells per cotyledon. Fig. 2B shows that at 2 dpg the total number of epidermal cells was similar in wild type and *axr3-1*. At 10 dpg, the total number of stomata/cotyledon was approximately five times higher in *axr3-1* than in the wild type (Fig. 2B). Notably, not only the number of stomata but also the number of non-stomatal cells increased strongly between 2 and 10 dpg in the *axr3-1* mutant, but not in the wild type (Fig. 2B). Similar results were obtained from the analysis of transgenic seedlings harbouring a *TMM::TMM-GFP* construct, which is expressed in meristemoids, GMCs and SLGCs (Nadeau and Sack, 2002), and can thus be used as a marker for incompletely differentiated stomatal lineage cells. In the wild-type background, only the number of GFP-positive cells increased significantly from 2 to 10 dpg, whereas the number of both GFP-positive and GFP-negative cells increased in the *axr3-1* background during this period (Fig. 2C).

To investigate the effects of the *axr3-1* mutation in the absence of cell division activity in the stomatal lineage, we analysed the *spch-3* mutant, which lacks entry into the stomatal lineage and therefore contains an epidermis solely composed of pavement cells (MacAlister et al., 2007). The total epidermal cell number did not increase between day 2 and day 10 after germination in *spch-3* (Fig. 2D). Similarly, in the *axr3-1 spch-3* double mutant, which is also devoid of stomata (see also below), the total epidermal cell number was essentially the same in 2-day- and 10-day-old seedlings, indicating no further cell division. These results demonstrate that the *axr3-1* mutation increases the total epidermal cell number (Fig. 2B) by enhancing cell division exclusively within the stomatal lineage. Hence, the higher number of non-stomatal cells in the *axr3-1* mutant is also solely a result of cell division activity in the stomatal lineage and, therefore, derived from SLGCs.

Auxin inhibits stomata formation

The stomata-overproducing phenotype of the auxin-insensitive mutants *axr2-1*, *axr3-1* and *shy2-2* suggests that auxin is involved in the regulation of stomatal development. To further test this hypothesis, we investigated the effect of exogenous auxin on stomata formation. In wild-type seedlings, concentrations of 10 µM or higher of the synthetic auxin 1-Naphthaleneacetic acid (NAA) strongly reduced the SI, an effect that was much weaker in *axr2-1*

Development (2014) 141, 3165-3176 doi:10.1242/dev.109181

and *axr3-1* (Fig. 3A; supplementary material Fig. S3). These results indicate that auxin inhibits stomatal development in a dosage-dependent manner. Reduction in the SI was accompanied by a reduction in the number of stomata as well as non-stomatal epidermal cells (Fig. 3B), thus further corroborating the hypothesis that auxin controls cell division in the stomatal lineage.

We subsequently analysed stomatal phenotypes of mutants with perturbed auxin biosynthesis or signalling. The *wei8 tar2* mutant with a defect in auxin biosynthesis (Stepanova et al., 2008) exhibited excessive stomata in darkness, similar to *axr3-1*, and occasionally formed clusters of two stomata in continuous white light (Wc) (Fig. 3D; supplementary material Fig. S4). *tir1 afb2 afb3* auxin receptor mutants exhibit variation in penetrance: class A seedlings are similar to the wild type, but have an agravitropic root and lack an apical hook in darkness; class B seedlings lack a root, form a rudimentary hypocotyl and often have only one cotyledon; class C seeds do not germinate (Dharmasiri et al., 2005b; Parry et al., 2009). Seedlings of classes A and B also differed in their stomatal phenotypes: dark-grown class A seedlings displayed a higher SI and formed both more stomata and more non-stomatal epidermal cells than the wild type, whereas class B seedlings showed not only more stomata in darkness but also clusters of two to three stomata (Fig. 3D,E; supplementary material Fig. S4). With the exception of this cluster formation, mutations in auxin biosynthesis and receptor genes affected stomata differentiation only in dark-grown and not in light-grown seedlings when compared with the wild type (Fig. 3D).

Many auxin-regulated processes require the establishment of auxin gradients via polar auxin transport (Tanaka et al., 2006). Dark-grown seedlings treated with the polar auxin transport inhibitor 1-N-naphthylphthalamic acid (NPA) showed an increased SI in darkness compared with the mock-treated control (Fig. 3C). This indicates that proper distribution of auxin via polar auxin transport is required for the suppression of stomatal development in darkness.

Auxin acts independently of brassinosteroids to suppress stomatal differentiation in darkness

BRs have recently been shown to regulate stomatal development (Gudesblat et al., 2012; Khan et al., 2013; Kim et al., 2012). Auxin and BRs are known to co-regulate light responses such as the shade avoidance response (Keller et al., 2011; Keuskamp et al., 2011).

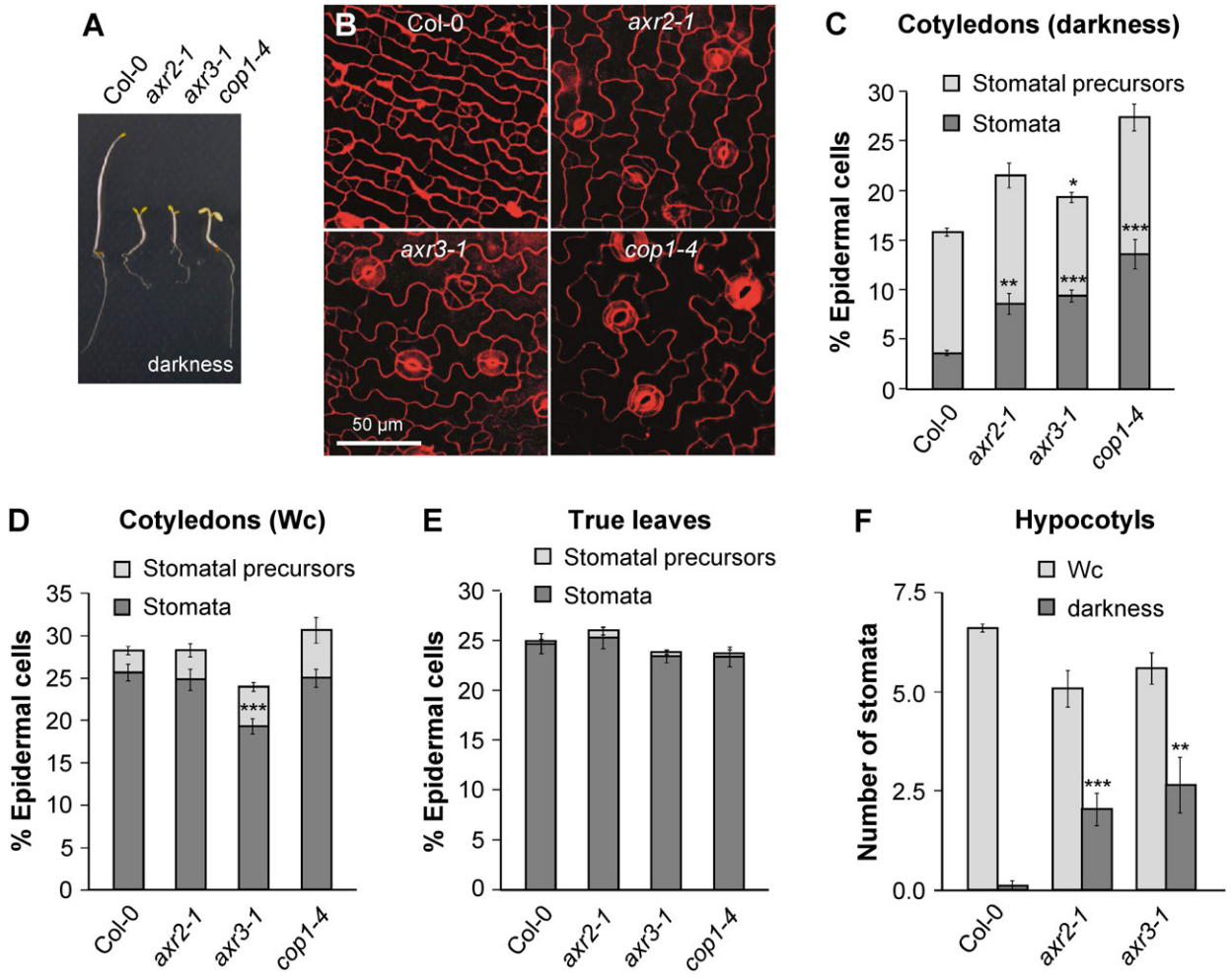

Fig. 1. The constitutively photomorphogenic mutants *axr2-1* and *axr3-1* form excessive stomata in darkness. (A) Visual phenotype of 4-day-old dark-grown seedlings of the indicated genotypes. (B) Confocal images of the cotyledon epidermis of dark-grown seedlings of the genotypes Col-0, *axr2-1*, *axr3-1* and *cop1-4*. Cell outlines were visualised by propidium iodide (PI) staining. Scale bar: 50 µm. (C-E) Quantification of stomata and stomatal precursors in the cotyledon epidermis of dark- (C) or white light (Wc)-grown (D) seedlings or in true leaves of 21-day-old adult plants (E). (F) Quantification of stomata in hypocotyls of dark- and Wc-grown seedlings of the indicated genotypes. Error bars represent s.e.m. Asterisks indicate significant differences in the proportion of stomatal precursors or stomata, respectively, when compared with the wild type (***P<0.001, **P<0.01, *P<0.05).

Development (2014) 141, 3165-3176 doi:10.1242/dev.109181

To test whether BRs and auxin interdependently regulate stomatal development, we tested the effect of NAA on stomata formation in combination with bikinin, an inhibitor of GSK3-like kinases in BR signalling (De Rybel et al., 2009). NAA and bikinin reduced the SI in the wild type and additive effects of both chemicals were evident in the *tmm-1* mutant. *axr3-1* was less responsive to NAA but still showed a wild type-like response to bikinin (supplementary material Fig. S5A-C). Moreover, auxin treatment could reduce the SI of the BR biosynthesis mutant *det2-1* (supplementary material Fig. S5D), suggesting that auxin does not act via BR biosynthesis to regulate stomatal development.

The stomata-overproducing phenotype of *axr3-1* depends on functional *SPCH*, *MUTE* and *FAMA*

SPCH, *MUTE* and *FAMA* are master regulators of consecutive steps in stomatal development. Loss of function of any of these genes results in the arrest of stomatal development at the step controlled by the respective gene: *spch* mutants display an epidermis completely devoid of stomata, whereas *mute* and *fama* mutants have arrested meristemoids and GMC clusters (‘*fama* tumours’), respectively (MacAlister et al., 2007; Ohashi-Ito and Bergmann, 2006; Pillitteri et al., 2007). To investigate genetic interactions of the *Aux*/*IAA* genes with *SPCH*, *MUTE* and *FAMA*, respective double mutants were generated. The cotyledon epidermis of dark-grown *axr3-1 spch-3* double mutants formed no stomata and, thus, exhibited the same phenotype as the *spch-3* single mutant (Fig. 4A). Hence, *SPCH* is required for expression of the *axr3-1* mutant phenotype. Phenotypes of the *axr3-1 mute-1* and *axr3-1 fama-1* double mutants also qualitatively resembled those of the respective *mute-1* and *fama-1* single mutants in that no guard cells were formed. Quantitatively, the proportions of meristemoids and ‘*fama* tumours’, respectively, were increased by the additional *axr3-1* mutation (Fig. 4A-C). This probably reflects an

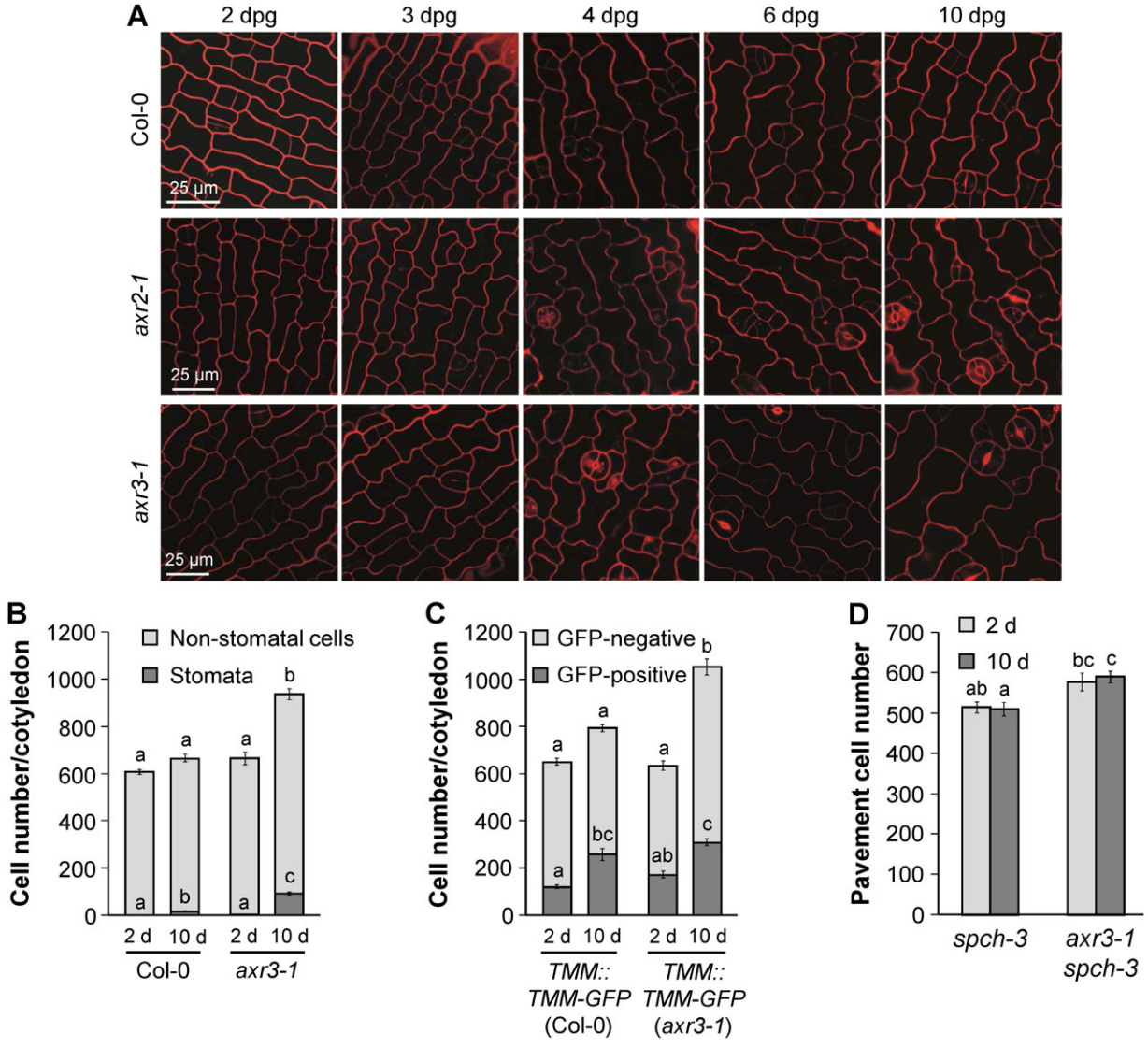

Fig. 2. The *axr3-1* mutant shows a post-embryonic increase in the division of stomatal lineage cells. (A) Confocal images of the cotyledon epidermis of dark-grown Col-0, *axr2-1* and *axr3-1* seedlings between 2 and 10 dpg. Cell outlines were visualised by PI staining. Scale bars: 25 µm. (B) Total number of mature stomata and non-stomatal cells (including stomatal precursors) in the cotyledon epidermis of 2- and 10-day-old dark-grown Col-0 and *axr3-1* seedlings. (C) Total number of GFP-positive and GFP-negative cells in the cotyledon epidermis of 2- and 10-day-old dark-grown Col-0 and *axr3-1* seedlings expressing a *TMM::TMM-GFP* construct. (D) Total number of pavement cells in the cotyledon epidermis of 2- and 10-day-old dark-grown *spch-3* and *axr3-1 spch-3* seedlings. Error bars denote s.e.m. Letters indicate significance groups for each cell type; samples with the same letters are not significantly different (P<0.05).

Development (2014) 141, 3165-3176 doi:10.1242/dev.109181

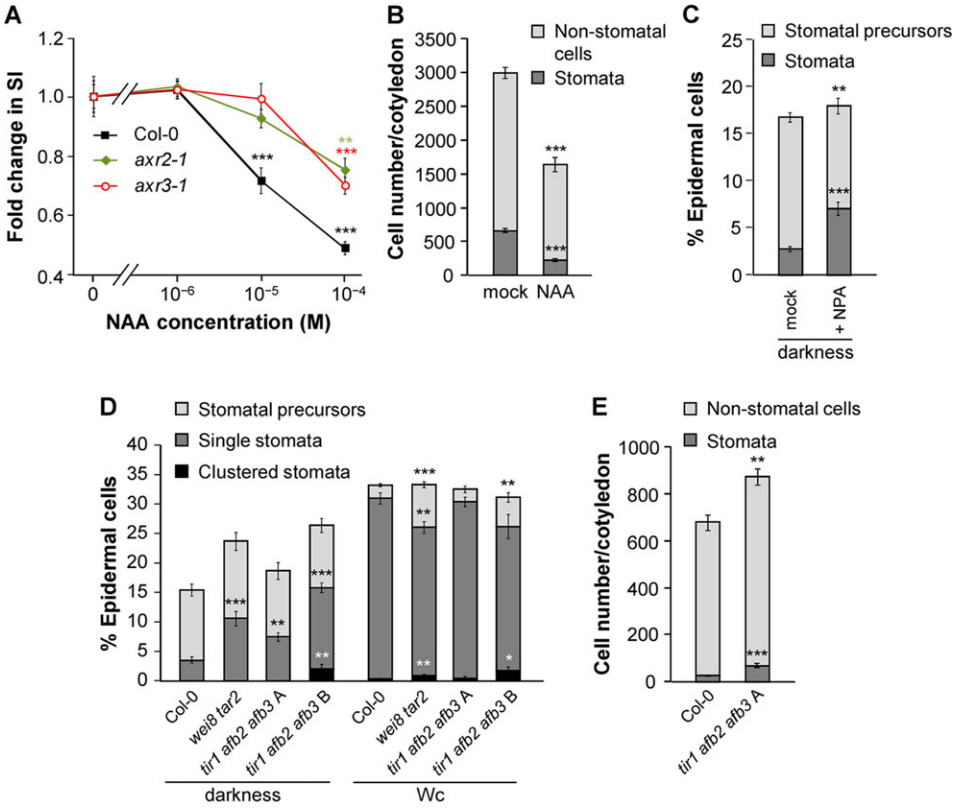

Fig. 3. Auxin affects stomatal development. (A) Fold change in the SI in the cotyledon epidermis of Wc-grown Col-0, *axr2-1* and *axr3-1* seedlings when treated with different concentrations of NAA. (B) Total number of stomata and non-stomatal cells (including stomatal precursors) in the cotyledon epidermis of Wc-grown seedlings treated with 10 µM NAA or mock treated. (C) Quantification of stomata and stomatal precursors in the cotyledon epidermis of seedlings treated with 10 µM NPA or mock treated. (D) Quantification of stomata and stomatal precursors in the cotyledon epidermis of the indicated genotypes. *tir1 afb2 afb3* triple mutant seedlings were grouped into classes A and B, which refer to mild and strong phenotypes, respectively. (E) Total number of stomata and non-stomatal cells in the cotyledon epidermis of dark-grown Col-0 and *tir1 afb2 afb3* triple mutant class A seedlings. Error bars represent s.e.m. Asterisks indicate significant differences in the proportion of the respective cell types when compared with the mock-treated control (A-C) and with the Col-0 wild type (D,E), respectively (***P<0.001, **P<0.01, *P<0.05).

increased entry of protodermal cells into the stomatal lineage in *axr3-1* mutants. Taken together, these observations suggest that *axr3-1* acts genetically upstream of the three *bHLH* genes and requires their function to enhance differentiation of mature stomata.

As the *axr3-1* phenotype depended on the three *bHLH* genes, we tested whether *axr3-1* affects their transcript levels. *SPCH, MUTE* and *FAMA* mRNA levels were only slightly elevated in dark-grown *axr2-1* and *axr3-1* mutants when compared with the wild type, whereas NAA treatment slightly reduced their expression in the wild type, but also in *axr3-1* (supplementary material Fig. S6). In dark-grown *cop1-4* mutants, in contrast, at least *SPCH* and *FAMA* transcript levels were much more strongly increased when compared with the wild type (Kang et al., 2009) (supplementary material Fig. S6). Thus, any major effect *axr3-1* might have on the three bHLH transcription factors is probably post-translational.

A constitutively active YDA MAPK cascade completely suppresses stomata formation in *axr3-1*

The YDA MAPK cascade acts upstream of SPCH, and probably also of MUTE and FAMA, to suppress stomatal development (Lampard et al., 2008; Ohashi-Ito and Bergmann, 2006; Pillitteri et al., 2007). It integrates signals from the light and BR signalling pathways (Kang et al., 2009; Khan et al., 2013; Kim et al., 2012), thus raising the possibility that it is also a downstream factor in AXR3 signalling.

Loss-of-function *yda* and *mpk3 mpk6* mutants as well as *MKK4-MKK5RNAi* plants have an epidermis consisting almost exclusively of stomata (Bergmann et al., 2004; Wang et al., 2007). Therefore, additional promoting effects of the *axr3-1* mutation would be difficult to detect in these backgrounds. By contrast, expression of constitutively active versions of YDA, MKK4 and MKK5 results in an epidermis completely devoid of stomata (Bergmann et al., 2004; Wang et al., 2007), but many lines expressing these constructs show strong silencing effects (Wang et al., 2007) and were thus not suitable for crossing and subsequent epistasis analysis. Instead, we crossed *axr3-1* into a *GVG*-Nt-*MEK2*^{DD} background harbouring a dexamethasone (DEX)-inducible construct of a constitutively active version of tobacco MEK2, which was shown to be functionally interchangeable with *Arabidopsis* MKK4 and MKK5 (Ren et al., 2002). This transgenic line was reported to reliably express the transgene in *Arabidopsis* (Wang et al., 2007). Both in the wild-type and the *axr3-1* background, induction of Nt-MEK2^{DD} expression resulted in the complete absence of stomata (Fig. 5), indicating that the positive effect of the *axr3-1* mutation on stomatal development cannot overcome the effect of a constitutively active YDA MAPK cascade. Therefore, *AXR3* appears to act genetically upstream of MPK3, MPK6, MKK4 and MKK5.

Genetic interactions between *axr3-1*, *tmm* and *er(l)* mutations

Upstream of the YDA MAPK cascade, TMM and ERf act cooperatively to restrict stomatal development (Bergmann et al., 2004; Lee et al., 2012; Shpak et al., 2005). To test whether AXR3 acts through these proteins to affect stomatal development, we investigated genetic interactions between *axr3-1*, *tmm-1* and various *er*(*l*) mutations.

When grown in the light, the *tmm-1* mutant exhibits a strong stomata-overproducing and clustering phenotype in leaves and cotyledons (Yang and Sack, 1995) (supplementary material Fig. S7A,B). In darkness, however, *tmm-1* hardly forms any mature stomata at all, but shows an increased proportion of meristemoids compared with the wild type (Kang et al., 2009) (Fig. 6A,B). This phenotype was drastically altered by an

Development (2014) 141, 3165-3176 doi:10.1242/dev.109181

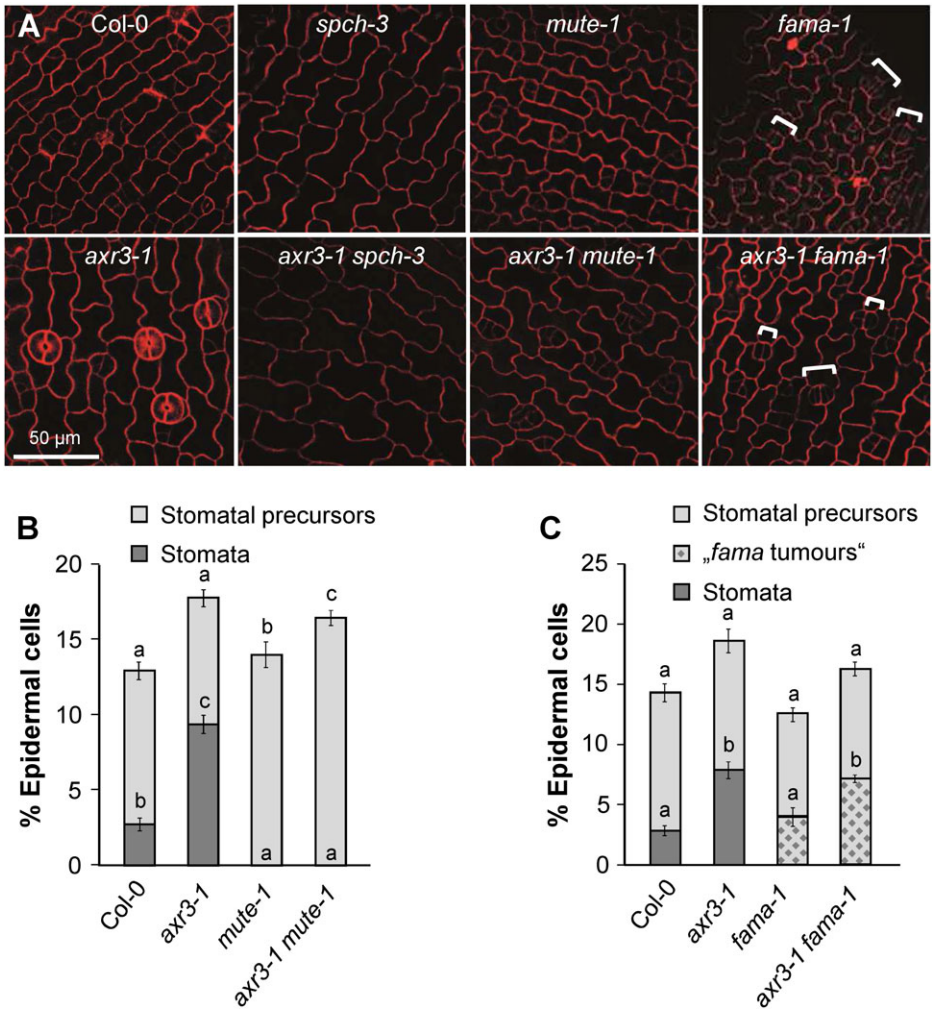

Fig. 4. The *axr3-1* mutation requires functional *SPCH*, *MUTE* and *FAMA* to promote stomatal development in darkness. (A) Confocal images of the cotyledon epidermis of 10-day-old dark-grown seedlings of the indicated genotypes. Cell outlines were visualised by PI staining. Square brackets highlight '*fama* tumours'. Scale bar: 50 µm. (B,C) Quantification of stomata, stomata precursors and '*fama* tumours' in the cotyledon epidermis of dark-grown seedlings of the indicated genotypes. Error bars indicate s.e.m. Letters indicate significance groups for each cell type; samples with the same letters are not significantly different (P<0.05).

additional *axr3-1* mutation: the *axr3-1 tmm-1* double mutant not only displayed a higher proportion of stomata than the *axr3-1* single mutant, but also developed stomatal clusters in darkness, which neither single mutant did (Fig. 6A,B). In the light, in contrast, the *axr3-1 tmm-1* stomatal phenotype was similar to the *tmm-1* single mutant (supplementary material Fig. S7A,B). Thus, the two mutations have synergistic effects in darkness, and *axr3-1* appears to provide a sensitised background in which lack of *TMM* causes the formation of stomatal clusters in darkness as well.

Different *ERf* genes affect different steps of stomatal development: in the light, *ER* primarily prevents entry divisions into the stomatal lineage, whereas *ERL1* predominantly inhibits subsequent development of stomatal precursors; *ERL2* has minor functions in both processes. A knock out of all three *ERf* genes results in a stomata-clustering phenotype that is even stronger than that of a *tmm* mutant (Shpak et al., 2005).

Functional divergence of *ERf* members was also seen in dark-grown seedlings: *er* and *er erl2* mutants showed an increased proportion of stomatal precursors when compared with the wild type, whereas *erl1* and *erl1 erl2* mutants formed more mature stomata than the wild type (Fig. 6C,D). Addition of the *axr3-1* mutation increased the proportion of stomata in each of these mutants, but to a lesser extent than in the wild-type background (Fig. 6C,D). Only a slight increase in clustered stomata due to *axr3-1* was detected in the *er erl1 erl2* triple mutant (Fig. 6C,E), and was only of low statistical significance in two experiments (P=0.085 for the experiment shown in Fig. 6E; P=0.046). Taken together, these results suggest that *axr3-1* acts – at least in part – through ERf proteins to affect stomatal development.

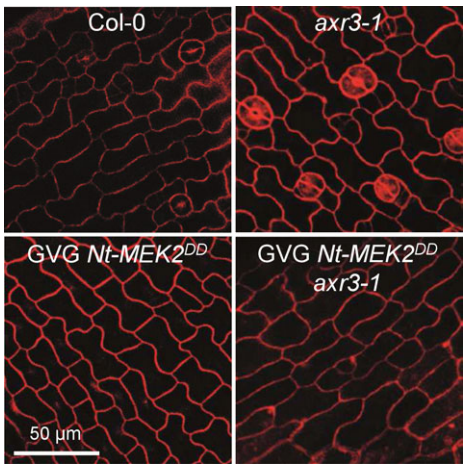

Fig. 5. A constitutively active MKK suppresses stomata formation in the *axr3-1* background. Confocal images of the cotyledon epidermis of dark-grown seedlings of Col-0 and *axr3-1* and of transgenic Col-0 and *axr3-1* seedlings expressing the DEX-inducible *GVG*-Nt-*MEK2*^{DD} construct. Seedlings were grown on medium supplemented with 0.02 µM DEX. Cell outlines were visualised by PI staining. Scale bar: 50 µm.

Development (2014) 141, 3165-3176 doi:10.1242/dev.109181

YDA and the ERf are important for the regulation of stomatal development by exogenous auxin and light

We subsequently investigated the auxin responsiveness of stomata patterning mutants. To this end, seedlings were grown on plates containing 10 µM NAA, a concentration that reduces the SI in the wild type (Fig. 3A and Fig. 7A). NAA treatment also reduced the SI in *epf1 epf2* and *tmm-1* mutants, whereas it had no significant effect in *er erl1 erl2* triple mutants and in loss-of-function *yda-10* mutants (Fig. 7A). Hence, the inhibitory effect of NAA on stomata formation was dependent on YDA and members of the ERf.

The effect of light/darkness on the stomatal phenotypes of the stomata-overproducing mutants was investigated as well. *yda-10* and *er erl1 erl2* also exhibited excessive stomata and stomata clusters in darkness, whereas the stomata-overproducing phenotypes of light-grown *tmm-1* and *epf1 epf2* were strongly attenuated when grown in darkness (Fig. 7B). As a consequence, stomata differentiation/clustering was more responsive to light in *epf1 epf2* and, in particular, in *tmm-1* mutants than in the wild type, *er erl1 erl2* and *yda-10* mutants.

As light and auxin seem to require the ERf to properly control stomatal development, we investigated whether the expression of the receptor-like kinases and their ligands of the *EPFL* family is altered in *axr* mutants or in NAA-treated seedlings. Transcript levels of *TMM*, all *ERf* members and several *EPFLs* were slightly elevated in dark-grown *axr* mutants when compared with the wild type (supplementary material Fig. S8A-D and Fig. S9A-D), but were not strongly affected by NAA treatment (supplementary material Figs S8E and S9E). Most of these genes act as negative regulators of stomatal development; it is thus unlikely that their elevated transcript levels are the cause for the stomatal phenotype of the *axr* mutants, but might rather be a consequence of the increased number of stomatal lineage cells.

COP1 and AXR3 act independently in suppressing stomata differentiation in darkness

Light affects stomatal development via inhibition of the COP1/SPA complex, and *COP1* has been shown to act genetically upstream of *YDA*, but in parallel with *TMM* (Kang et al., 2009). Thus, *axr3-1* and *cop1* mutations exhibit similar genetic interactions with mutations in stomata patterning genes. The *axr3-1 cop1-4* double mutant produced a larger fraction of stomata than either single mutant (Fig. 8A,B), suggesting that both genes act in independent pathways. This is further corroborated by the fact that neither COP1 protein levels nor its subcellular localisation were changed in dark-grown *axr2-1* and *axr3-1* mutants when compared with the wild type (supplementary material Fig. S10A,B). Furthermore, the

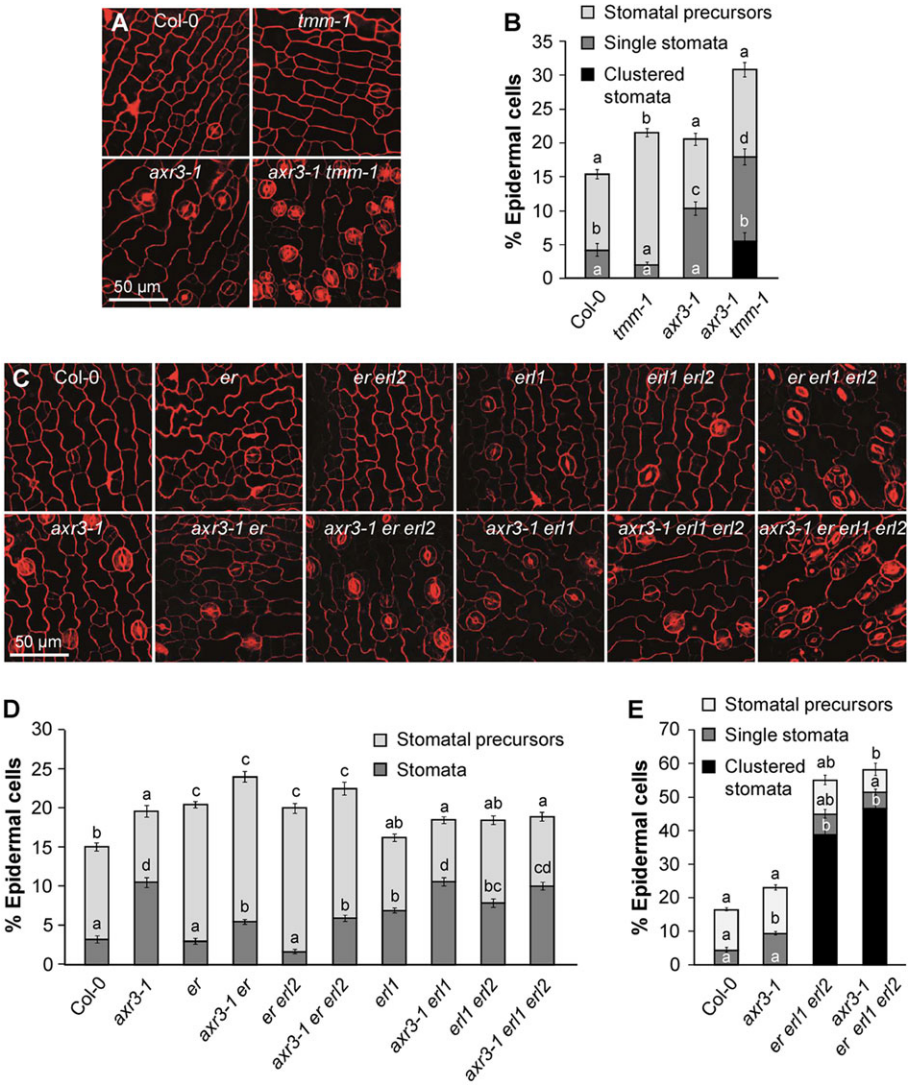

Fig. 6. The *axr3-1* mutation shows additive and synergistic effects with loss-of-function mutations in *TMM* and genes of the *ERf*. (A,C) Confocal images of the cotyledon epidermis of dark-grown seedlings of the indicated genotypes. Cell outlines were visualised by PI staining. Scale bars: 50 µm. (B,D,E) Quantification of stomata and stomatal precursors of the genotypes shown in A and C, respectively. Error bars represent s.e.m. Letters indicate significance groups for each cell type; samples with the same letters are not significantly different (P<0.05).

Development (2014) 141, 3165-3176 doi:10.1242/dev.109181

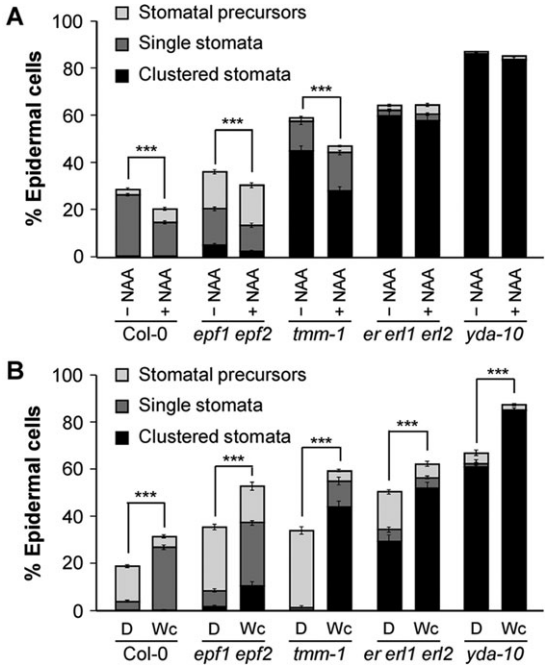

Fig. 7. Effects of auxin and light on stomatal development are attenuated in *yda* and *er erl1 erl2* mutants. (A) Quantification of stomata and stomatal precursors in the cotyledon epidermis of Wc-grown seedlings of the indicated genotypes when treated with 10 µM NAA or mock treated. (B) Quantification of stomata and stomatal precursors in the cotyledon epidermis of dark- and Wc-grown seedlings of the same genotypes as in A. Error bars represent s.e.m. Asterisks denote significant differences between the proportion of mature stomata (=percentage of clustered+single stomata) in the indicated genotypes (***P<0.001, **P<0.01, *P<0.05).

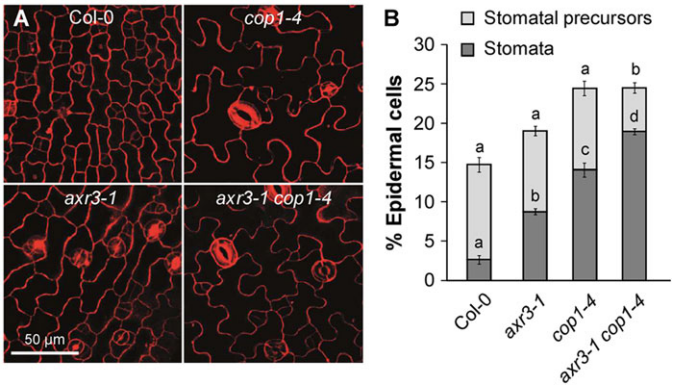

Fig. 8. *axr3-1* and *cop1-4* have additive effects on stomatal development. (A) Confocal images of the cotyledon epidermis of dark-grown seedlings of the indicated genotypes. Cell outlines were visualised by PI staining. Scale bar: 50 µm. (B) Quantification of stomata and stomatal precursors of the genotypes shown in A. Error bars represent s.e.m. Letters indicate significance groups for each cell type; samples with the same letters are not significantly different (P<0.05).

transcript levels of *AXR2*, *AXR3* and *SHY2* in dark-grown *cop1-4* mutants were not significantly different from those detected in the wild type (supplementary material Fig. S10C).

Besides COP1, PHYTOCHROME INTERACTING FACTORS (PIFs) represent key players in the light signalling pathway (Leivar and Quail, 2011); PIF4 has also been shown to promote stomatal development in response to high intensities of red light (Casson et al., 2009) and might thus also play a role in the regulation of stomata formation in darkness. *PIF4* transcript levels were significantly reduced in dark-grown *axr3-1* and *axr2-1* mutants when compared with the wild type, but were not affected by NAA treatment of light-grown seedlings (supplementary material Fig. S11). Although the activity of PIF4 in seedlings is thus far unknown, it appears that *PIF4* transcript levels do not fully correlate with the stomata phenotypes under the conditions tested.

Expression of *axr3-1-YFP* in the epidermis partially mimics the *axr3-1* mutant phenotype

The *axr3-1* mutation requires the stomatal signalling pathway to promote stomata differentiation; however, it is unclear in which cell type the axr3-1 protein acts. To address this, the *axr3-1* mutant coding sequence fused to *YFP* was expressed under different cell type-specific promoters in the wild-type background. The set of promoters used comprised the *35S* and *AXR3* promoters, the *MERISTEM LAYER1* (*ML1*) promoter for epidermal specificity (Sessions et al., 1999), the *CHLOROPHYLL A/B BINDING PROTEIN3* (*CAB3*) promoter for mesophyll specificity (Susek et al., 1993) and the *SPCH* and *ICE1* promoters for specificity to the stomatal lineage. *SPCH* is expressed broadly in the protoderm in leaf primordia, but its expression is restricted to MMCs and young meristemoids later in development (MacAlister et al., 2007), whereas the *ICE1* expression domain encompasses meristemoids, GMCs, young guard cells and SLGCs (Kanaoka et al., 2008).

No transgenic plants with visible AXR3-1-YFP accumulation were found among those transformed with the *35S::axr3-1-YFP* construct, implying that ubiquitous expression of the AXR3-1 mutant protein is lethal. Furthermore, most T1 plants expressing *axr3-1-YFP* from the *CAB3* or *ICE1* promoter did not set seed; therefore, none of the *CAB3::axr3-1-YFP* and only two of the *ICE1::axr3-1-YFP* lines could be propagated and analysed.

In dark-grown *AXR3::axr3-1-YFP* seedlings, a YFP signal was detected in epidermal and cortical cells of the hypocotyl, in the upper part of the root and, in some lines, also in pavement cells close to the margin of the cotyledons, but no YFP signal was detected in stomatal lineage cells of the abaxial cotyledon epidermis in any of the lines analysed (Fig. 9A-C; supplementary material Fig. S12 top panel). Accumulation of AXR3-1-YFP in pavement cells and stomatal lineage cells was found in dark-grown *ML1::axr3-1-YFP* seedlings (Fig. 9E; supplementary material Fig. S12 middle panel). The *SPCH::axr3-1-YFP* lines accumulated AXR3-1-YFP weakly in pavement cells and most strongly in small cells that lacked any sign of differentiation and often occurred in pairs (Fig. 9G; supplementary material Fig. S12 bottom panel), a pattern that was also observed for transcriptional and translational SPCH reporters (MacAlister et al., 2007). The YFP signal in the epidermis of *ICE1::axr3-1-YFP* lines was restricted to meristemoids, GMCs and cells adjacent to these (Fig. 9I; supplementary material Fig. S12 bottom panel). No YFP signal was detected in the mesophyll in any line expressing *axr3-1-YFP* (Fig. 9D,F,H,J).

All transgenic *axr3-1-YFP* lines were analysed for whether they mimic the *axr3-1* stomatal phenotype in dark-grown seedlings. The *AXR3::axr3-1-YFP* lines showed a significantly higher SI than the wild type, although it was slightly lower than the SI of the *axr3-1* mutant (Fig. 9K). A significant increase in the SI was also observed for all *ML1::axr3-1-YFP* lines, except for line 3-4. By contrast, seedlings expressing *axr3-1-YFP* from the *SPCH* and *ICE1* promoters exhibited an SI similar to the wild type. Hence, expression of *axr3-1-YFP* in the stomatal lineage was insufficient to promote stomata formation, thus implying that AXR3-1 acts non-cell-autonomously.

Development (2014) 141, 3165-3176 doi:10.1242/dev.109181

We also investigated whether other facets of the *axr3-1* mutant phenotype were observed in the *axr3-1-YFP* lines. The short hypocotyl phenotype of a dark-grown *axr3-1* mutant was mimicked by all *AXR3::axr3-1-YFP* lines (supplementary material Fig. S13A,B). Two *ML1::axr3-1-YFP* and one *SPCH::axr3-1-YFP* line also showed a reduction in hypocotyl length when compared with the wild type, but to a much lesser extent. All of the *ICE1::axr3-1-YFP* lines appeared similar to the wild type (supplementary material Fig. S13A,B). The vegetative growth phenotype of the *axr3-1* mutant, characterised by dwarfism and leaf hyponasty, was not mimicked entirely by any transgenic line. Four *AXR3::axr3-1-YFP* lines, however, were dwarfed compared with the wild type and also displayed hyponastic leaves (supplementary material Fig. S14). Expression of *axr3-1-YFP* from the *ML1* and *SPCH* promoters caused leaf epinasty and reduced plant size. Hence, AXR3-1-YFP can have opposite effects on leaf curvature when expressed in different tissues. *ICE1::axr3-1-YFP* lines appeared similar to the wild type.

DISCUSSION

Light strongly promotes the differentiation of stomata in cotyledons and leaves, which is consistent with the role of stomata in photosynthetic gas exchange. It has been shown previously that photoreceptors, the COP1/SPA complex and PIF proteins are involved in light-regulated stomatal development (Boccalandro et al., 2009; Casson et al., 2009; Kang et al., 2009). Here, we have identified auxin as an important regulator that suppresses stomata differentiation in dark-grown seedlings. Moreover, we have placed AXR3 within the genetic signalling network that regulates stomatal development in response to intrinsic and external signals. Taken together with a recent report demonstrating the important role of polar auxin transport and auxin distribution in stomatal patterning of light-grown seedlings (Le et al., 2014), our results support the notion that auxin is a negative regulator of stomatal differentiation.

Auxin via AUX/IAA proteins inhibits stomata differentiation in dark-grown seedlings

Several lines of evidence indicate that auxin and nuclear auxin signalling repress stomata formation in darkness: first, we have shown that the *aux/iaa* gain-of-function mutants *shy2-2*, *axr2-1* and *axr3-1*, which are resistant to auxin, produce more stomata in hypocotyls and cotyledons of dark-grown seedlings when compared with the wild type. Second, exogenous application of NAA reduces the SI in the wild type, but less in *axr3-1* mutant seedlings. Third, mutants that are either defective in auxin biosynthesis or in auxin perception via the

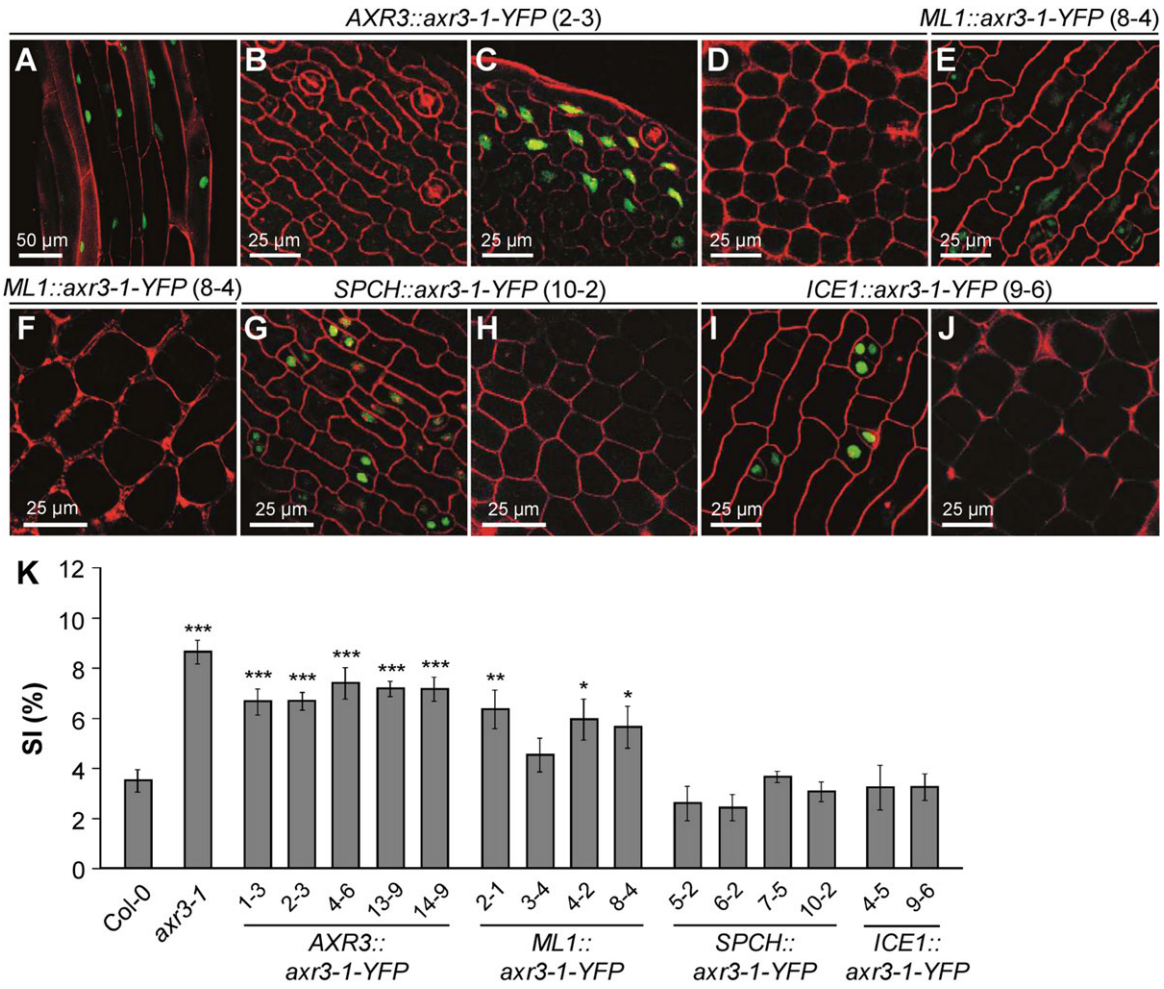

Fig. 9. Expression of *axr3-1-YFP* exclusively in the epidermis increases the SI. (A-J) Confocal images of the hypocotyl (A), the cotyledon epidermis (B,C,E,G,I) and the cotyledon mesophyll (D,F,H,J) showing the accumulation of AXR3-1-YFP protein in transgenic seedlings expressing the fusion genes from the indicated promoters. Scale bars: 50 µm in A, 25 µm in B-J. (K) SI of the cotyledon epidermis of dark-grown seedlings of the indicated *promoter::axr3-1-YFP* lines. Numbers denote independent transgenic lines. Error bars represent s.e.m. Asterisks indicate significant differences to the wild type (***P<0.001, **P<0.01, *P<0.05).

Development (2014) 141, 3165-3176 doi:10.1242/dev.109181

TIR1/ABF auxin receptor family show an enhanced production of stomata in darkness similar to the auxin-resistant *axr* mutants. Hence, genetic perturbance on any level, either auxin biosynthesis, auxin perception or auxin signalling, led to a de-repression of stomata formation in dark-grown seedlings. Genetic lesions in auxin biosynthesis or signalling affected the SI exclusively in dark-grown, but not in light-grown seedlings. Auxin signalling is thus required to suppress stomata differentiation primarily in darkness. However, light-grown *wei8 tar2* seedlings show weak stomatal clustering, and strongly penetrant *tir1 afb2 afb3* mutant seedlings produce stomata clusters at a similar frequency in the light and in darkness. The formation of excessive clusters has also been recently reported for the *tir1 afb1 afb2 afb3* quadruple mutant (Le et al., 2014). Hence, auxin has a dual role in stomata differentiation: a dark-dependent role in suppressing stomata formation without an apparent function in stomata spacing, and a possibly light-independent role in maintaining proper spacing of stomata.

Light can affect auxin levels, distribution and responsiveness. Increased auxin biosynthesis and polar auxin transport are crucial events during the shade avoidance growth response to a low red/far-red ratio (Casal, 2012; Tao et al., 2008), a condition that also reduces stomata differentiation (Boccalandro et al., 2009; Casson and Hetherington, 2014). The molecular mechanisms underlying the effect of auxin on the morphogenesis of a dark-grown seedling are, in contrast, poorly understood. It appears unlikely that light prevents auxin-dependent suppression of stomatal development by reducing overall auxin levels, because these levels are lower in dark-grown than in light-grown seedlings, at least when examining the whole shoot tissue of a seedling (Bhalerao et al., 2002). However, although polar auxin transport is not required for hypocotyl elongation in darkness (Jensen et al., 1998), auxin transport might influence local auxin concentrations in cells of the stomatal lineage, as was recently demonstrated for light-grown seedlings (Le et al., 2014). Consistent with this idea, our results show that NPA treatment also led to excessive stomata in dark-grown seedlings, although without forming stomata clusters. Interestingly, long-distance signalling also controls stomatal differentiation in response to light intensity, as shading of a mature leaf causes a reduction in the SI of an unshaded young leaf (Casson and Hetherington, 2014; Lake et al., 2001).

The *axr3-1* mutation promotes cell division in the stomatal lineage of dark-grown seedlings

The observed increase in the SI in dark-grown auxin-resistant seedlings could principally be the result of a reduced number of pavement cells and/or an increased number of stomata. Our analysis of total cell numbers in *axr3-1* cotyledons and in *axr3-1 spch* cotyledons lacking a stomatal lineage clearly indicates that the *axr3-1* mutation increases cell division activity exclusively in the stomatal lineage, thereby also producing excess pavement cells derived from SLGCs. Hence, the increase in the SI in dark-grown *axr3-1* mutant seedlings is associated with an increase in cell division activity in the stomatal lineage post germination. This suggests that the consistent changes of total cell numbers observed in *tir1 afb2 afb3* seedlings and in NAA-treated wild-type seedlings are also a result of changes in cell division activity exclusively in the stomatal lineage. The *axr3-1* mutation appears to also cause a very slight, although statistically non-significant, increase in total cell numbers in 2-day-old dark-grown cotyledons, i.e. prior to stomata differentiation. Therefore, we cannot fully exclude the possibility that disruption of auxin signalling also increases cell division activity during embryogenesis or very early after seed imbibition.

Two pieces of evidence suggest that a disruption of auxin signalling by the *axr3-1* mutation promotes both the entry divisions into the stomatal lineage and the differentiation of stomatal precursors into mature guard cells. First, dark-grown *axr3-1* mutants exhibit a higher number of mature stomata without decreasing the proportion of stomatal precursor cells. Second, the *axr3-1* mutation increases the number of meristemoids and '*fama*-tumours' in the *mute-1* and *fama-1* backgrounds, respectively. This demonstrates that if progression through the stomatal lineage is arrested by *mute* or *fama* mutations, *axr3-1* still increases entry divisions into the stomatal lineage. Hence, we suggest that the *axr3-1* mutation enhances the cell division-promoting activity of the bHLH transcription factors. However, we also consider it possible that the *axr3-1* mutation, moreover, enhances cell division activity in the stomatal lineage by promoting earlier cell divisions that provide cells for the stomatal lineage. Taken together, it appears that proper auxin signalling is required for the inhibition of at least two transitions in stomatal differentiation in darkness. Auxin levels dynamically change during stomatal patterning of light-grown seedlings and thereby direct the switch from unequal to equal cell division (Le et al., 2014). An analysis of auxin activity using reporter lines might resolve auxin action on cell division patterns in dark-grown seedlings.

Although the effect of *axr3-1* on stomatal development requires the presence of the stomatal lineage, expression of an *axr3-1-YFP* fusion gene from stomatal lineage-specific promoters (*SPCH*, *ICE1*) did not mimic the stomatal phenotype of the *axr3-1* mutant. Hence, action of the AXR3-1 protein in stomatal lineage cells was not sufficient to promote stomata formation. Instead, these results suggest that AXR3-1 also acts outside of the stomatal lineage to promote divisions within the stomatal lineage, implying that cell-cell communication is involved in this process.

A genetic network for the control of stomatal development that integrates intrinsic and external signals

Epistasis analysis revealed that *axr3-1* requires functional *SPCH*, *MUTE* and *FAMA* genes to promote stomata formation in dark-grown seedlings, suggesting that auxin and auxin signalling act upstream of these transcription factors. The effect of *axr3-1* also requires a functional YDA MAPK cascade, thus placing *AXR3* upstream of this MAPK cascade. This is supported by the failure of exogenous NAA to reduce the SI in an *yda* loss-of-function mutant.

axr3-1 exhibits synergistic effects with *tmm-1*, suggesting that *AXR3* and *TMM* do not act in a common linear signalling pathway, but that mutations in *AXR3* or *TMM* mutually sensitise components of the signalling pathways for the respective loss of the other. The *axr3-1* mutation shows additive interactions with mutations in *ERf* genes. However, the effect of *axr3-1* was reduced in an *er erl1 erl2* triple mutant background, implying that *axr3-1* might act at least in part via the ERf to affect stomatal development in darkness. In agreement with this idea, auxin-induced reduction in stomata formation was abolished in *er erl1 erl2* mutants. Hence, the YDA MAPK cascade, possibly via ERf proteins, is a likely target of auxin and auxin signalling in the regulation of stomatal development. Interestingly, auxin treatment was shown to activate a MAPK cascade in *Arabidopsis* roots, and it has been suggested that this induction is independent of stress associated with this treatment (Mockaitis and Howell, 2000). Apart from the EPFL-ERf pathway (Jewaria et al., 2013; Lee et al., 2012), the YDA MAPK cascade also integrates signals from the BR signalling cascade (Khan et al., 2013; Kim et al., 2012) and the light signalling pathway (Kang et al., 2009). Thus, the YDA MAPK cascade is a central switch

Development (2014) 141, 3165-3176 doi:10.1242/dev.109181

responding to intrinsic and environmental signals in the decision of whether or not to form a stoma.

MATERIALS AND METHODS

Plant material

axr2-1 (Timpte et al., 1994), *axr3-1* (Leyser et al., 1996), *cop1-4* (Deng and Quail, 1992), *det2-1* (Chory et al., 1991), *epf1-1 epf2-3* (Hara et al., 2009), *er-105* (Torii et al., 1996), *er-105 erl1-2 erl2-1*, *er-105 erl2-1*, *erl1-2*, *erl1-2 erl2-1* (all Shpak et al., 2004), *fama-1* (Ohashi-Ito and Bergmann, 2006), *mute-1* (Pillitteri et al., 2007), *shy2-2* (Reed et al., 1998), *spch-3* (MacAlister et al., 2007), *tir1-1 afb2-3 afb3-4* (Parry et al., 2009), *tmm-1* (Yang and Sack, 1995), *wei8-1 tar2-1* (Stepanova et al., 2008) and *yda-10* (Kang et al., 2009) as well as the transgenic lines *GVG*-Nt*MEK2*^{DD} (Ren et al., 2002) and *TMM::TMM-GFP* (Nadeau and Sack, 2002) have been described previously. All *axr3-1* genotypes used for epistasis analysis were generated by crossing and were confirmed using the primers listed in supplementary material Table S1.

Plant growth

Light sources and general growth conditions have been described previously (Laubinger et al., 2004). Seedlings were grown in darkness or Wc (25 µM m^{-2} s^{-1}) on MS medium containing 1% (w/v) sucrose. For NAA treatment, medium was supplemented with various concentrations of NAA. For treatment with NPA, DEX and bikinin, medium was supplemented with 10 µM NPA, 0.02 µM DEX and 30 µM bikinin, respectively, or the equivalent amounts of DMSO for mock treatment.

Microscopy

For observation by bright-field microscopy, seedlings were cleared in chloral hydrate solution as described by Kang et al. (2009) and analysed using an Eclipse E800 compound light microscope (Nikon Instruments). For confocal microscopy, samples were stained in 10 µg/ml PI for several minutes and then mounted in water. They were visualised by a DM5500Q confocal laser-scanning microscope (Leica Microsystems).

Quantification of epidermal cells

For quantification of epidermal cells, calculation of the percentage of stomata/stomatal precursors and subsequent statistical analysis see supplementary materials and methods.

Plasmid construction and selection of transgenic plants

For generation of *promoter::axr3-1-YFP* constructs, see supplementary materials and methods. Constructs were transformed into Col-0 wild type, and 30-40 independent transgenic lines were analysed for each construct. Four to five representative lines showing a 3:1 segregation of the resistance marker and correct cell type-specific accumulation of the AXR3-1-YFP fusion protein were propagated further to obtain homozygous transgenic lines.

Real-time PCR, total protein preparation and nuclear fractionation

Purification of total RNA, qPCR, total protein isolation and nuclear fractionation of proteins have been described previously (Balcerowicz et al., 2011). Primers used for qPCR are listed in supplementary material Table S2.

Acknowledgements

We thank Dominique Bergmann, Mark Estelle, Fred Sack, Keiko Torii, Paul Overvoorde, José Alonso and Shuqun Zhang for sharing seeds of mutants and transgenic lines. We are grateful to George Coupland for providing promoter entry clones, to Robert Hänsch for providing the pDest-Venus-GW-Ter vector and to Francois Ouellet for providing the pBS-axr3-1 vector. We thank Florian Kreische, Monique Henschel, Johannes Stauber and Vicky Tilmes for excellent technical assistance, and Klaus Menrath and the greenhouse staff for expert care of our plants.

Competing interests

The authors declare no competing financial interests.

Author contributions

The project was designed by U.H. and M.B. Most experiments were conducted by M.B. A.R. performed the initial characterisation of the *axr3-1* mutant stomata phenotype. L.R. genotyped and characterised mutants used for epistasis analysis. G.F. generated transgenic axr3-1-YFP plants. M.B. and U.H. wrote the manuscript, with all other authors commenting on it.

Funding

This research was supported by the Deutsche Forschungsgemeinschaft [SFB572 and SFB590] and the University of Cologne to U.H. A.R. held a fellowship from the International Graduate School for Genetics and Functional Genomics at the University of Cologne.

Supplementary material

Supplementary material available online at
http://dev.biologists.org/lookup/suppl/doi:10.1242/dev.109181/-/DC1

References

Balcerowicz, M., Fittinghoff, K., Wirthmueller, L., Maier, A., Fackendahl, P., Fiene, G., Koncz, C. and Hoecker, U. (2011). Light exposure of Arabidopsis seedlings causes rapid de-stabilization as well as selective post-translational inactivation of the repressor of photomorphogenesis SPA2. *Plant J.* **65**, 712-723.

Bergmann, D. C., Lukowitz, W. and Somerville, C. R. (2004). Stomatal development and pattern controlled by a MAPKK kinase. *Science* **304**, 1494-1497.

Bhalerao, R. P., Eklöf, J., Ljung, K., Marchant, A., Bennett, M. and Sandberg, G. (2002). Shoot-derived auxin is essential for early lateral root emergence in Arabidopsis seedlings. *Plant J.* **29**, 325-332.

Bhave, N. S., Veley, K. M., Nadeau, J. A., Lucas, J. R., Bhave, S. L. and Sack, F. D. (2009). TOO MANY MOUTHS promotes cell fate progression in stomatal development of Arabidopsis stems. *Planta* **229**, 357-367.

Boccalandro, H. E., Rugnone, M. L., Moreno, J. E., Ploschuk, E. L., Serna, L., Yanovsky, M. J. and Casal, J. J. (2009). Phytochrome B enhances photosynthesis at the expense of water-use efficiency in Arabidopsis. *Plant Physiol.* **150**, 1083-1092.

Casal, J. J. (2012). Shade avoidance. *Arab. Book Am. Soc. Plant Biol.* **10**, e0157.

Casson, S. A. and Hetherington, A. M. (2014). phytochrome B is required for light-mediated systemic control of stomatal development. *Curr. Biol.* **24**, 1216-1221.

Casson, S. A., Franklin, K. A., Gray, J. E., Grierson, C. S., Whitelam, G. C. and Hetherington, A. M. (2009). phytochrome B and PIF4 regulate stomatal development in response to light quantity. *Curr. Biol.* **19**, 229-234.

Chory, J., Nagpal, P. and Peto, C. A. (1991). Phenotypic and genetic analysis of det2, a new mutant that affects light-regulated seedling development in Arabidopsis. *Plant Cell* **3**, 445-459.

De Rybel, B., Audenaert, D., Vert, G., Rozhon, W., Mayerhofer, J., Peelman, F., Coutuer, S., Denayer, T., Jansen, L., Nguyen, L. et al. (2009). Chemical inhibition of a subset of Arabidopsis thaliana GSK3-like kinases activates brassinosteroid signalling. *Chem. Biol.* **16**, 594-604.

Deng, X.-W. and Quail, P. H. (1992). Genetic and phenotypic characterization of cop1 mutants of Arabidopsis thaliana. *Plant J.* **2**, 83-95.

Dharmasiri, N., Dharmasiri, S. and Estelle, M. (2005a). The F-box protein TIR1 is an auxin receptor. *Nature* **435**, 441-445.

Dharmasiri, N., Dharmasiri, S., Weijers, D., Lechner, E., Yamada, M., Hobbie, L., Ehrismann, J. S., Jürgens, G. and Estelle, M. (2005b). Plant development is regulated by a family of auxin receptor F box proteins. *Dev. Cell* **9**, 109-119.

Gray, W. M., Kepinski, S., Rouse, D., Leyser, O. and Estelle, M. (2001). Auxin regulates SCF^{TIR1}-dependent degradation of AUX/IAA proteins. *Nature* **414**, 271-276.

Gudesblat, G. E., Schneider-Pizoń, J., Betti, C., Mayerhofer, J., Vanhoutte, I., van Dongen, W., Boeren, S., Zhiponova, M., de Vries, S., Jonak, C. et al. (2012). SPEECHLESS integrates brassinosteroid and stomata signalling pathways. *Nat. Cell Biol.* **14**, 548-554.

Hara, K., Yokoo, T., Kajita, R., Onishi, T., Yahata, S., Peterson, K. M., Torii, K. U. and Kakimoto, T. (2009). Epidermal cell density is autoregulated via a secretory peptide, EPIDERMAL PATTERNING FACTOR 2 in Arabidopsis leaves. *Plant Cell Physiol.* **50**, 1019-1031.

Hayashi, K.-I. (2012). The interaction and integration of auxin signalling components. *Plant Cell Physiol.* **53**, 965-975.

Jensen, P. J., Hangarter, R. P. and Estelle, M. (1998). Auxin transport is required for hypocotyl elongation in light-grown but not dark-grown Arabidopsis. *Plant Physiol.* **116**, 455-462.

Jewaria, P. K., Hara, T., Tanaka, H., Kondo, T., Betsuyaku, S., Sawa, S., Sakagami, Y., Aimoto, S. and Kakimoto, T. (2013). Differential effects of the peptides stomagen, EPF1 and EPF2 on activation of MAP kinase MPK6 and the SPCH protein level. *Plant Cell Physiol.* **54**, 1253-1262.

Kanaoka, M. M., Pillitteri, L. J., Fujii, H., Yoshida, Y., Bogenschutz, N. L., Takabayashi, J., Zhu, J.-K. and Torii, K. U. (2008). SCREAM/ICE1 and

SCREAM2 specify three cell-state transitional steps leading to Arabidopsis stomatal differentiation. *Plant Cell* **20**, 1775-1785.
Kang, C.-Y., Lian, H.-L., Wang, F.-F., Huang, J.-R. and Yang, H.-Q. (2009). Cryptochromes, phytochromes, and COP1 regulate light-controlled stomatal development in Arabidopsis. *Plant Cell* **21**, 2624-2641.
Keller, M. M., Jaillais, Y., Pedmale, U. V., Moreno, J. E., Chory, J. and Ballaré, C. L. (2011). Cryptochrome 1 and phytochrome B control shade-avoidance responses in Arabidopsis via partially independent hormonal cascades. *Plant J.* **67**, 195-207.
Kepinski, S. and Leyser, O. (2005). The Arabidopsis F-box protein TIR1 is an auxin receptor. *Nature* **435**, 446-451.
Keuskamp, D. H., Sasidharan, R., Vos, I., Peeters, A. J. M., Voesenek, L. A. C. J. and Pierik, R. (2011). Blue-light-mediated shade avoidance requires combined auxin and brassinosteroid action in Arabidopsis seedlings. *Plant J.* **67**, 208-217.
Khan, M., Rozhon, W., Bigeard, J., Pflieger, D., Husar, S., Pitzschke, A., Teige, M., Jonak, C., Hirt, H. and Poppenberger, B. (2013). Brassinosteroid-regulated GSK3/shaggy-like kinases phosphorylate Mitogen-activated Protein (MAP) kinase kinases, which control stomata development in Arabidopsis thaliana. *J. Biol. Chem.* **288**, 7519-7527.
Kim, T.-W., Michniewicz, M., Bergmann, D. C. and Wang, Z.-Y. (2012). Brassinosteroid regulates stomatal development by GSK3-mediated inhibition of a MAPK pathway. *Nature* **482**, 419-422.
Lake, J. A., Quick, W. P., Beerling, D. J. and Woodward, F. I. (2001). Plant development: signals from mature to new leaves. *Nature* **411**, 154.
Lampard, G. R., MacAlister, C. A. and Bergmann, D. C. (2008). Arabidopsis stomatal initiation is controlled by MAPK-mediated regulation of the bHLH SPEECHLESS. *Science* **322**, 1113-1116.
Lampard, G. R., Lukowitz, W., Ellis, B. E. and Bergmann, D. C. (2009). Novel and expanded roles for MAPK signalling in Arabidopsis stomatal cell fate revealed by cell type-specific manipulations. *Plant Cell* **21**, 3506-3517.
Laubinger, S., Fittinghoff, K. and Hoecker, U. (2004). The SPA quartet: a family of WD-repeat proteins with a central role in suppression of photomorphogenesis in Arabidopsis. *Plant Cell* **16**, 2293-2306.
Le, J., Liu, X.-G., Yang, K.-Z., Chen, X.-L., Zou, J.-J., Wang, H.-Z., Wang, M., Vanneste, S., Morita, M., Tasaka, M. et al. (2014). Auxin transport and activity regulate stomatal patterning and development. *Nat. Commun.* **5, 3090**.
Lee, J. S., Kuroha, T., Hnilova, M., Khatayevich, D., Kanaoka, M. M., McAbee, J. M., Sarikaya, M., Tamerler, C. and Torii, K. U. (2012). Direct interaction of ligand-receptor pairs specifying stomatal patterning. *Genes Dev.* **26**, 126-136.
Leivar, P. and Quail, P. H. (2011). PIFs: pivotal components in a cellular signalling hub. *Trends Plant Sci.* **16**, 19-28.
Leyser, H. M. O., Pickett, F. B., Dharmasiri, S. and Estelle, M. (1996). Mutations in the AXR3 gene of Arabidopsis result in altered auxin response including ectopic expression from the SAUR-AC1 promoter. *Plant J.* **10**, 403-413.
MacAlister, C. A., Ohashi-Ito, K. and Bergmann, D. C. (2007). Transcription factor control of asymmetric cell divisions that establish the stomatal lineage. *Nature* **445**, 537-540.
Mockaitis, K. and Howell, S. H. (2000). Auxin induces mitogenic activated protein kinase (MAPK) activation in roots of Arabidopsis seedlings. *Plant J.* **24**, 785-796.
Nadeau, J. A. and Sack, F. D. (2002). Control of stomatal distribution on the Arabidopsis leaf surface. *Science* **296**, 1697-1700.
Ohashi-Ito, K. and Bergmann, D. C. (2006). Arabidopsis FAMA controls the final proliferation/differentiation switch during stomatal development. *Plant Cell* **18**, 2493-2505.
Parry, G., Calderon-Villalobos, L. I., Prigge, M., Peret, B., Dharmasiri, S., Itoh, H., Lechner, E., Gray, W. M., Bennett, M. and Estelle, M. (2009). Complex regulation of the TIR1/AFB family of auxin receptors. *Proc. Natl. Acad. Sci. USA* **106**, 22540-22545.
Pillitteri, L. J. and Torii, K. U. (2012). Mechanisms of stomatal development. *Annu. Rev. Plant Biol.* **63**, 591-614.
Pillitteri, L. J., Sloan, D. B., Bogenschutz, N. L. and Torii, K. U. (2007). Termination of asymmetric cell division and differentiation of stomata. *Nature* **445**, 501-505.
Reed, J. W. (2001). Roles and activities of Aux/IAA proteins in Arabidopsis. *Trends Plant Sci.* **6**, 420-425.
Reed, J. W., Elumalai, R. P. and Chory, J. (1998). Suppressors of an Arabidopsis thaliana phyB mutation identify genes that control light signalling and hypocotyl elongation. *Genetics* **148**, 1295-1310.
Ren, D., Yang, H. and Zhang, S. (2002). Cell death mediated by MAPK is associated with hydrogen peroxide production in Arabidopsis. *J. Biol. Chem.* **277**, 559-565.
Rychel, A. L., Peterson, K. M. and Torii, K. U. (2010). Plant twitter: ligands under 140 amino acids enforcing stomatal patterning. *J. Plant Res.* **123**, 275-280.
Sessions, A., Weigel, D. and Yanofsky, M. F. (1999). The Arabidopsis thaliana MERISTEM LAYER 1 promoter specifies epidermal expression in meristems and young primordia. *Plant J.* **20**, 259-263.
Shpak, E. D., Berthiaume, C. T., Hill, E. J. and Torii, K. U. (2004). Synergistic interaction of three ERECTA-family receptor-like kinases controls Arabidopsis organ growth and flower development by promoting cell proliferation. *Development* **131**, 1491-1501.
Shpak, E. D., McAbee, J. M., Pillitteri, L. J. and Torii, K. U. (2005). Stomatal patterning and differentiation by synergistic interactions of receptor kinases. *Science* **309**, 290-293.
Stepanova, A. N., Robertson-Hoyt, J., Yun, J., Benavente, L. M., Xie, D.-Y., Doležal, K., Schlereth, A., Jürgens, G. and Alonso, J. M. (2008). TAA1-mediated auxin biosynthesis is essential for hormone crosstalk and plant development. *Cell* **133**, 177-191.
Susek, R. E., Ausubel, F. M. and Chory, J. (1993). Signal transduction mutants of Arabidopsis uncouple nuclear CAB and RBCS gene expression from chloroplast development. *Cell* **74**, 787-799.
Tan, X., Calderon-Villalobos, L. I. A., Sharon, M., Zheng, C., Robinson, C. V., Estelle, M. and Zheng, N. (2007). Mechanism of auxin perception by the TIR1 ubiquitin ligase. *Nature* **446**, 640-645.
Tanaka, H., Dhonukshe, P., Brewer, P. B. and Friml, J. (2006). Spatiotemporal asymmetric auxin distribution: a means to coordinate plant development. *Cell. Mol. Life Sci.* **63**, 2738-2754.
Tao, Y., Ferrer, J.-L., Ljung, K., Pojer, F., Hong, F., Long, J. A., Li, L., Moreno, J. E., Bowman, M. E., Ivans, L. J. et al. (2008). Rapid synthesis of auxin via a new tryptophan-dependent pathway is required for shade avoidance in plants. *Cell* **133**, 164-176.
Timpte, C., Wilson, A. K. and Estelle, M. (1994). The axr2-1 mutation of Arabidopsis thaliana is a gain-of-function mutation that disrupts an early step in auxin response. *Genetics* **138**, 1239-1249.
Tiwari, S. B., Wang, X.-J., Hagen, G. and Guilfoyle, T. J. (2001). AUX/IAA proteins are active repressors, and their stability and activity are modulated by auxin. *Plant Cell* **13**, 2809-2822.
Torii, K. U., Mitsukawa, N., Oosumi, T., Matsuura, Y., Yokoyama, R., Whittier, R. F. and Komeda, Y. (1996). The Arabidopsis ERECTA gene encodes a putative receptor protein kinase with extracellular leucine-rich repeats. *Plant Cell* **8**, 735-746.
Ulmasov, T., Hagen, G. and Guilfoyle, T. J. (1999). Activation and repression of transcription by auxin-response factors. *Proc. Natl. Acad. Sci. USA* **96**, 5844-5849.
Wang, H., Ngwenyama, N., Liu, Y., Walker, J. C. and Zhang, S. (2007). Stomatal development and patterning are regulated by environmentally responsive mitogen-activated protein kinases in Arabidopsis. *Plant Cell* **19**, 63-73.
Wengier, D. L. and Bergmann, D. C. (2012). On fate and flexibility in stomatal development. *Cold Spring Harb. Symp. Quant. Biol.* **77**, 53-62.
Yang, M. and Sack, F. D. (1995). The too many mouths and four lips mutations affect stomatal production in Arabidopsis. *Plant Cell* **7**, 2227-2239.

Supplementary Materials and Methods

Quantification of epidermal cell types

Epidermal cell types were quantified in bright field images of cleared cotyledons of 10-d-old seedlings or leaves of 21-d-old plants using ImageJ 1.43u software (Wayne Rasband, NIH, Bethesda, USA). Depending on cotyledon or leaf size, up to three areas in the abaxial epidermis were selected, avoiding the margin and the area close to the petiole, and cell types in these areas were counted. Area size was 250 µm x 250 µm in cotyledons of light-grown seedlings and 100 µm x 100 µm in cotyledons of dark-grown seedlings. Epidermal cells were classified as stomata (i.e. pairs of guard cells), stomatal precursors (i.e. meristemoids and GMCs) or other epidermal cells according to morphological differences described in Nadeau and Sack (2002). Percentage of stomata was calculated as stomata / (stomata + stomatal precursors + other epidermal cells) and percentage of stomatal precursors was calculated as stomatal precursors / (stomata + stomatal precursors + other epidermal cells).

For quantification of total cell numbers, cells were quantified in confocal images of whole, PI-stained cotyledons of 2- or 10-d-old seedlings using ImageJ 1.43 software. For light-grown seedlings, cells in one half of each cotyledon were counted and the total cell numbers were extrapolated.

Eight to ten cotyledons or leaves of individual seedlings and plants, respectively, were analysed per genotype and condition. Percentages of stomata and stomatal precursors were calculated for each cotyledon or leaf individually before mean and s.e.m. were calculated from these data.

Statistical analysis

Statistical analyses were performed in R (http://www.r-project.org). Data were checked for deviations from normality using the Shapiro-Wilk test. Variances of normally distributed data were then analysed using Levene's test for homogeneity of variance. Comparisons of two normally distributed samples with equal variances were carried out using a two-tailed *t*-test; in case of unequal variances a Welch-corrected *t*-test was applied. For multiple comparisons of normally distributed data, an ANOVA (or Welch-ANOVA for samples with unequal variances) was performed. If significant differences were detected by ANOVA, a post-hoc

analysis was carried out using Tukey's HSD test for samples with equal variances or Dunnett's modified Tukey-Kramer test for samples with unequal variances.

In rare cases when data showed strong deviations from a normal distribution, non-parametric tests were performed. For pairwise comparisons, a Wilcoxon rank sum test was used while for multiple comparisons, a Kruskal-Wallis one-way analysis of variance was carried out, which was followed by multiple pairwise Wilcoxon rank sum tests if significant differences were detected.

Plasmid construction

To generate *promoter::axr3-1-YFP* constructs the Venus-YFP coding sequence was PCR-amplified from the pDEST-Venus-GW-Ter vector (R. Hänsch, unpublished) with primers introducing XhoI and SpeI restriction sites, the purified PCR product was digested with XhoI and SpeI and ligated into pJIC30 (Corbesier et al., 2007), thereby generating pJIC30-YFP. The *axr3-1* ORF was PCR-amplified from the pBS-axr3-1 vector (Ouellet et al., 2001) with primers introducing HindIII and XhoI restriction sites, the purified PCR product was digested with HindIII and XhoI and ligated into pJIC30-YFP, thereby generating pJIC30-axr3-1-YFP.

Promoter fragments 2421 bp upstream of the *AXR3* ORF, 2581 bp upstream of the *ICE1* ORF and 2574 bp upstream of the *SPCH* ORF were amplified from Col-0 genomic DNA and the purified PCR products were cloned into pDONR^{TM}207 using GATEWAY® BP technology, thereby generating the promoter entry clones pDONR^{TM}207-AXR3pro, pDONR^{TM}207-ICE1pro and pDONR^{TM}207-SPCHpro. Entry clones containing the *ML1* and *CAB3* promoters were described previously (An et al., 2004; Ranjan et al., 2011). *Promoter::axr3-1-YFP* constructs were generated by GATEWAY® LR reactions between these promoter entry clones and the pJIC30-axr3-1-YFP destination vector. Primers used for cloning are listed in Table S3.

Supplementary References

An, H., Roussot, C., Suárez-López, P., Corbesier, L., Vincent, C., Piñeiro, M., Hepworth, S., Mouradov, A., Justin, S., Turnbull, C., et al. (2004). CONSTANS acts in the phloem to regulate a systemic signal that induces photoperiodic flowering of Arabidopsis. *Development* **131**, 3615–3626.

Corbesier, L., Vincent, C., Jang, S., Fornara, F., Fan, Q., Searle, I., Giakountis, A., Farrona, S., Gissot, L., Turnbull, C., et al. (2007). FT Protein Movement

Contributes to Long-Distance Signaling in Floral Induction of Arabidopsis. *Science* **316**, 1030–1033.

Nadeau, J. A. and Sack, F. D. (2002). Stomatal Development in Arabidopsis. *Arabidopsis Book* **1**, e0066.

Ouellet, F., Overvoorde, P. J. and Theologis, A. (2001). IAA17/AXR3: Biochemical Insight into an Auxin Mutant Phenotype. *Plant Cell* **13**, 829–841.

Ranjan, A., Fiene, G., Fackendahl, P. and Hoecker, U. (2011). The Arabidopsis repressor of light signaling SPA1 acts in the phloem to regulate seedling de-etiolation, leaf expansion and flowering time. *Development* **138**, 1851–1862.

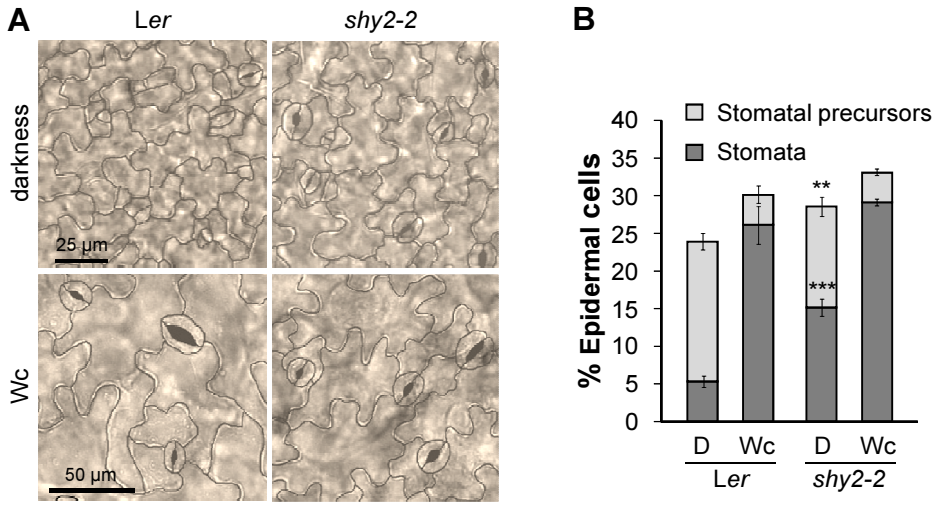

Fig. S1. The *shy2-2* mutant shows increased stomata formation in darkness. (**A**) Brightfield images of the cotyledon epidermis of dark- and Wc-grown seedlings of the indicated genotypes. Cell outlines were traced in dark grey. (**B**) Quantification of stomata and stomata precursors of the genotypes shown in A. Error bars represent the s.e.m. Asterisks indicate indicate significant differences in the proportion of stomatal precursors or stomata, respectively, when compared to the L*er* wild type (*** $p < 0.001$, ** $p < 0.01$, * $p < 0.05$).

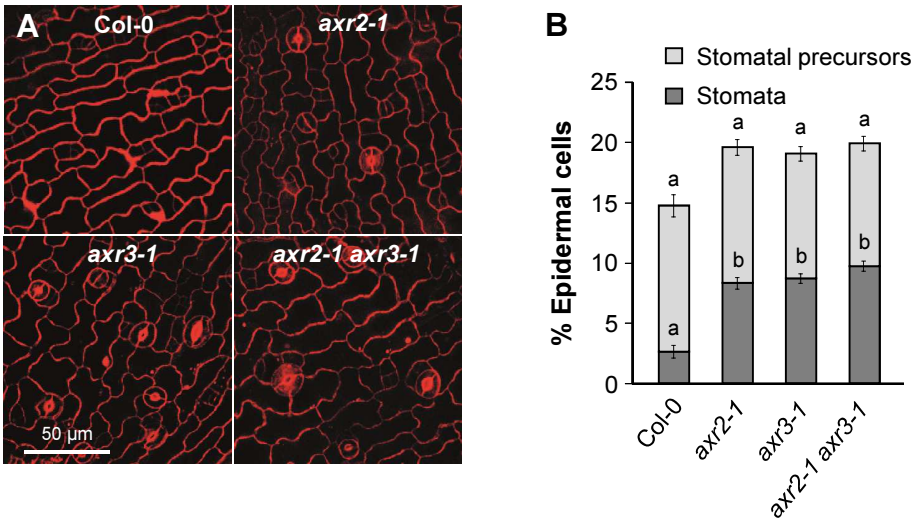

Fig. S2. The *axr2-1 axr3-1* double mutant shows no increased stomata formation in comparison to the respective single mutants. (**A**) Confocal images of the cotyledon epidermis of dark-grown seedlings of the indicated genotypes. Cell outlines were visualised by PI staining. (**B**) Quantification of stomata and stomatal precursors of the genotypes shown in A. Error bars represent the s.e.m. Letters indicate significance groups for each cell type; samples with the same letters are not significantly different ($p < 0.05$).

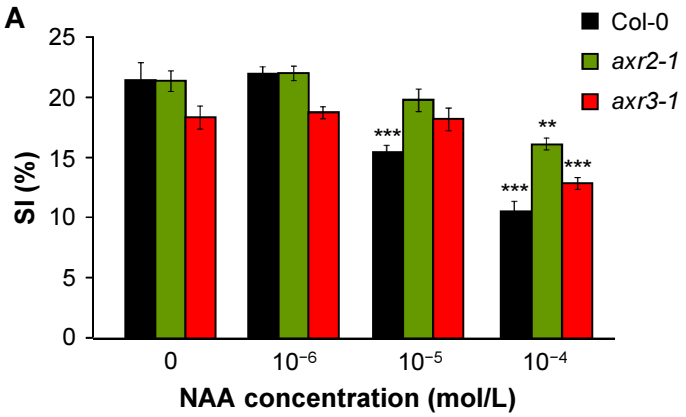

Fig. S3. NAA treatment affects stomatal development. SI of the cotyledon epidermis of Wc-grown Col-0, *axr2-1* and *axr3-1* seedlings treated with different concentrations of NAA. Error bars represent the s.e.m. Asterisks indicate significant differences to the wild type (*** $p < 0.001$, ** $p < 0.01$, * $p < 0.05$).

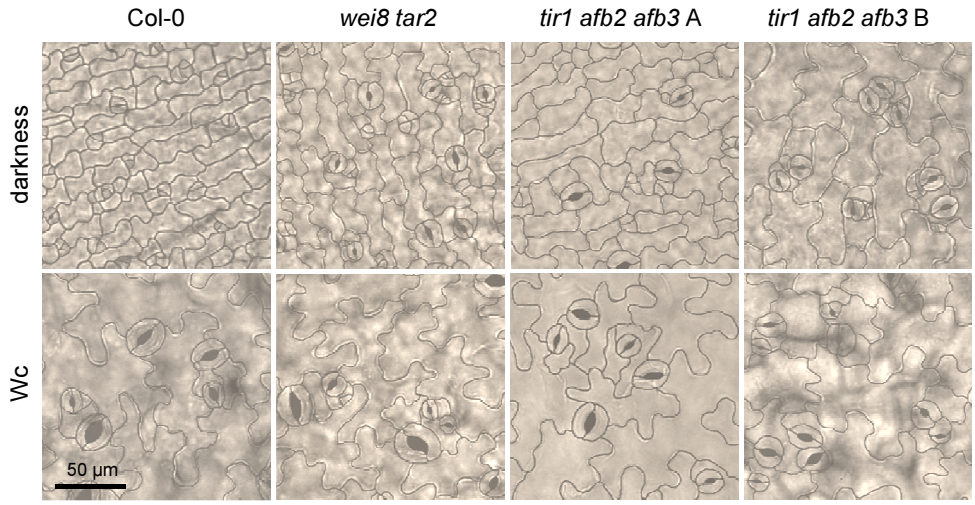

Fig. S4. Mutants deficient in auxin biosynthesis or auxin perception are defective in stomatal development. Brightfield images of the cotyledon epidermis of dark- and Wc-grown seedlings of the indicated genotypes. *tir1 afb2 afb3* seedlings were grouped into classes A and B, which refer to mild and strong phenotypes, respectively. Cell outlines were traced in dark grey.

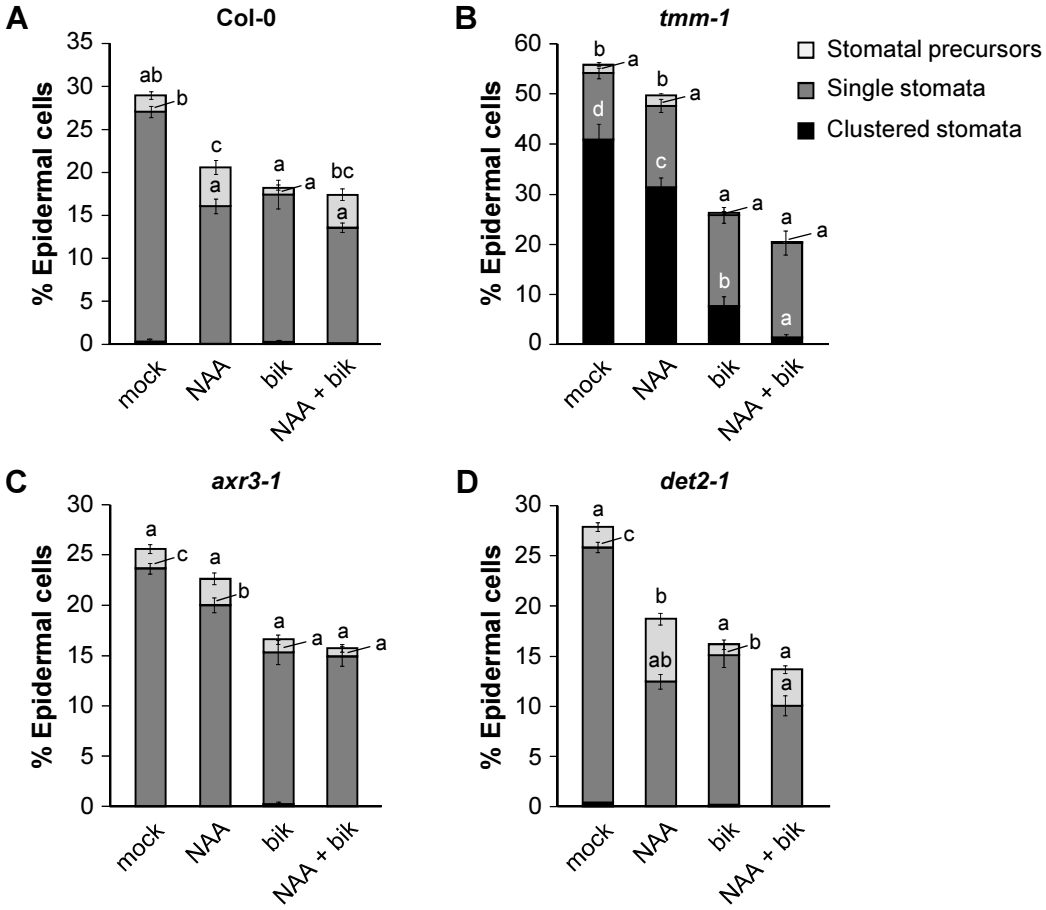

Fig. S5. NAA and bikinin have additive effects on stomata formation. Quantification of stomata and stomatal precursors in the abaxial cotyledon epidermis of Wc-grown Col-0 (A), *tmm-1* (B), *axr3-1* (C) and *det2-1* (D) seedlings treated with 10 µM NAA, 30 µM bikinin, a combination of both or mock-treated. Error bars represent the s.e.m. Letters indicate significance groups for each cell type; samples with the same letters are not significantly different ($p < 0.05$).

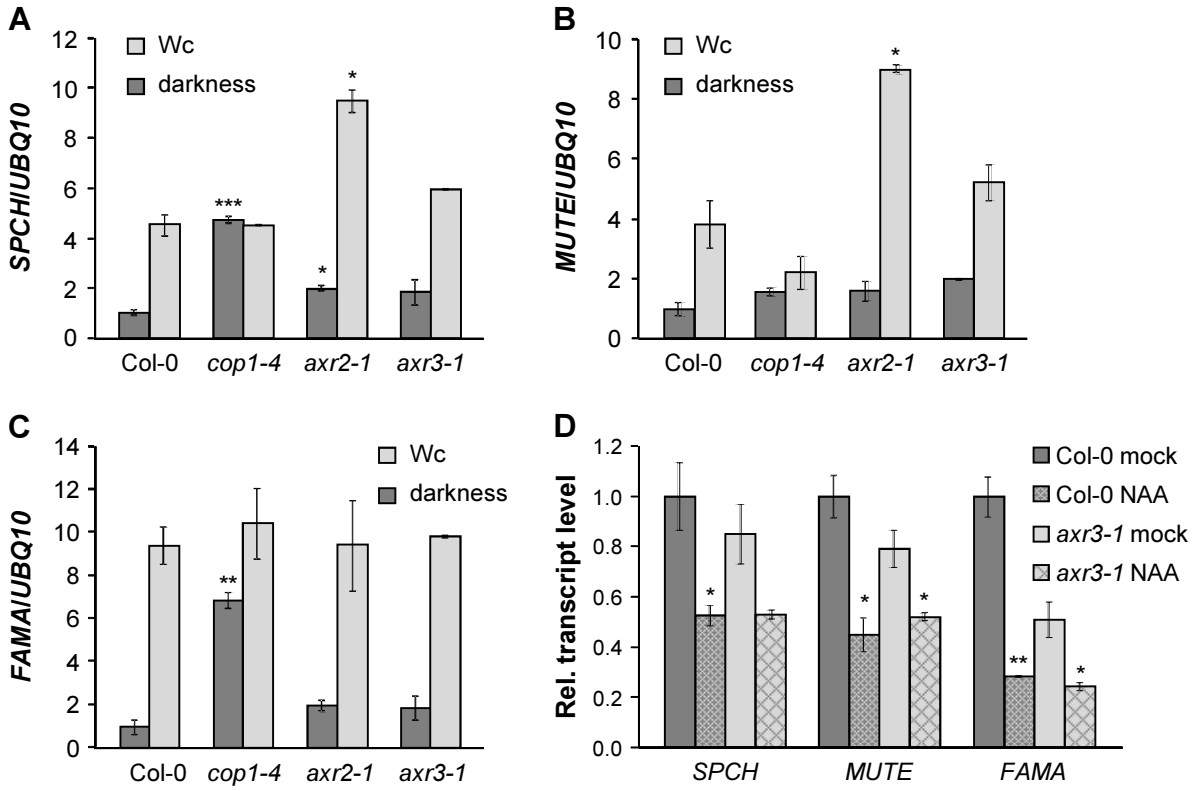

Fig. S6. Analysis of *SPCH*, *MUTE* and *FAMA* transcripts. (**A-C**) Transcript levels of *SPCH* (A), *MUTE* (B) and *FAMA* (C) in 5-d-old dark- or Wc-grown seedlings of the indicated genotypes. (**D**) *SPCH*, *MUTE* and *FAMA* transcript levels in 5-d-old Wc-grown Col-0 and *axr3-1* seedlings treated with 10 µM NAA or mock-treated. Transcript levels were normalised to *UBQ10* and are shown relative to the levels of dark-grown Col-0 seedlings (A-C) or the mock-treated Col-0 control (D). Error bars represent the s.e.m. Asterisks indicate significant differences to dark-grown wild type (A-C) or the mock-treated control (D) (*** $p < 0.001$, ** $p < 0.01$, * $p < 0.05$).

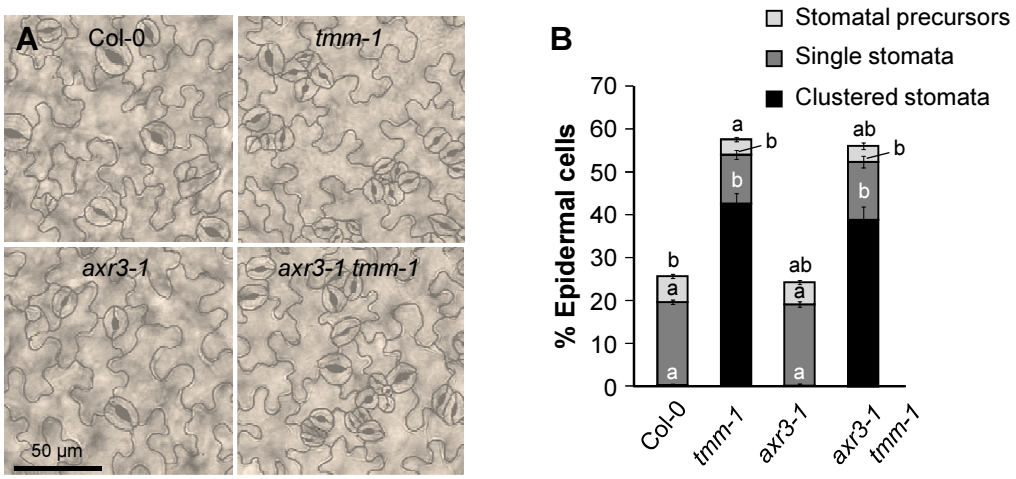

Fig. S7: The *axr3-1* mutation has no effect on the phenotype of Wc-grown *tmm-1* mutant seedlings. (**A**) Brightfield images of the cotyledon epidermis of Wc-grown seedlings of the indicated genotypes. Cell outlines were traced in dark grey. (**B**) Quantification of stomata and stomatal precursors of the genotypes shown in A. Error bars represent the s.e.m. Letters indicate significance groups for each cell type; samples with the same letters are not significantly different ($p < 0.05$).

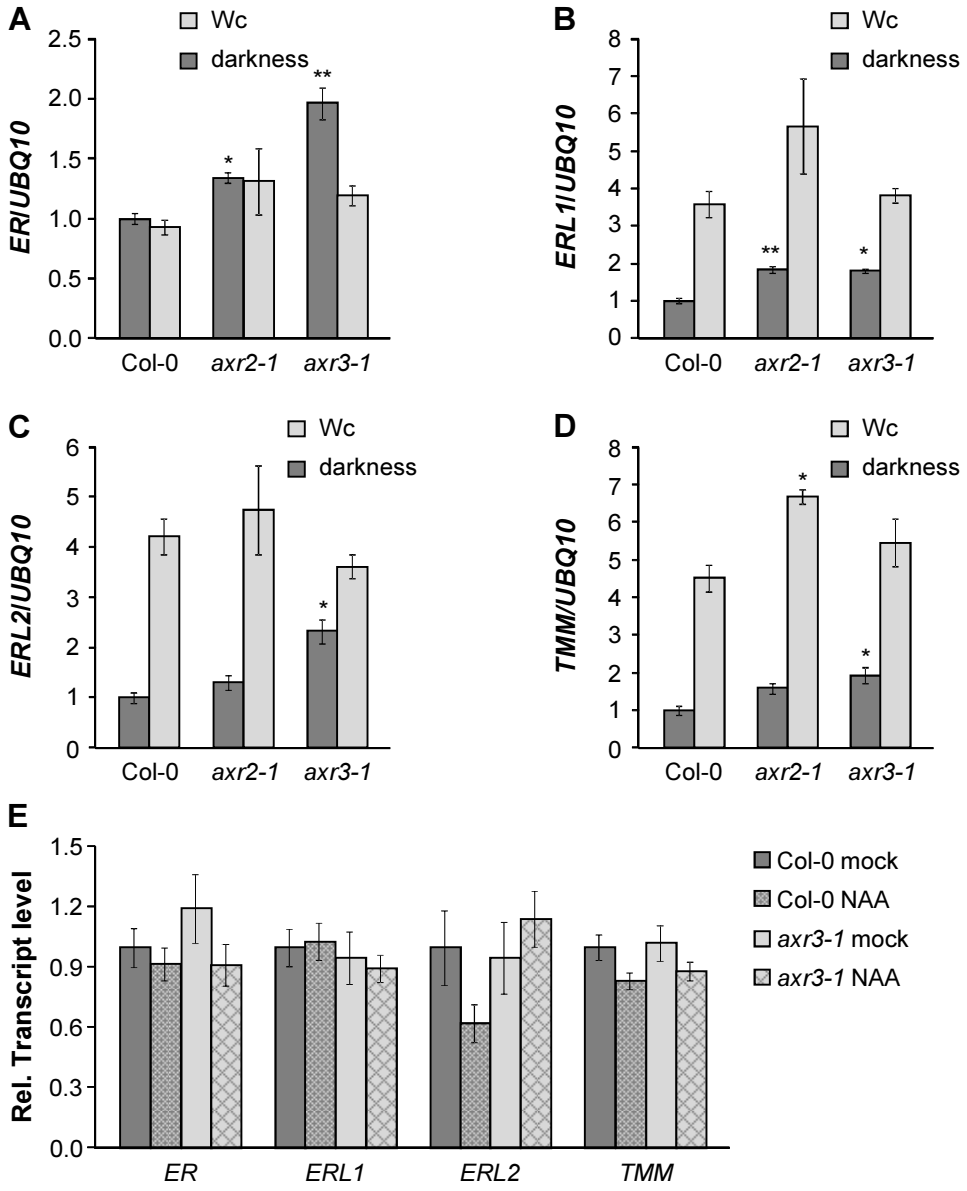

Fig. S8. Analysis of *ER*(*L*) *and TMM* transcripts. (**A-D**) Transcript levels of *ER* (A), *ERL1* (B), *ERL2* (C) and *TMM* (D) in 5-d-old dark- or Wc-grown seedlings of the indicated genotypes. (**E**) *ER*(*L*) and *TMM* transcript levels in 5-d-old Wc-grown Col-0 and *axr3-1* seedlings treated with 10 µM NAA or mock-treated. Transcript levels were normalised to *UBQ10* and are shown relative to the levels of dark-grown Col-0 seedlings (A-D) or the mock-treated Col-0 control (E). Error bars represent the s.e.m. Asterisks indicate significant differences to dark-grown wild type (A-D) or the mock-treated control (E) (*** $p < 0.001$, ** $p < 0.01$, * $p < 0.05$).

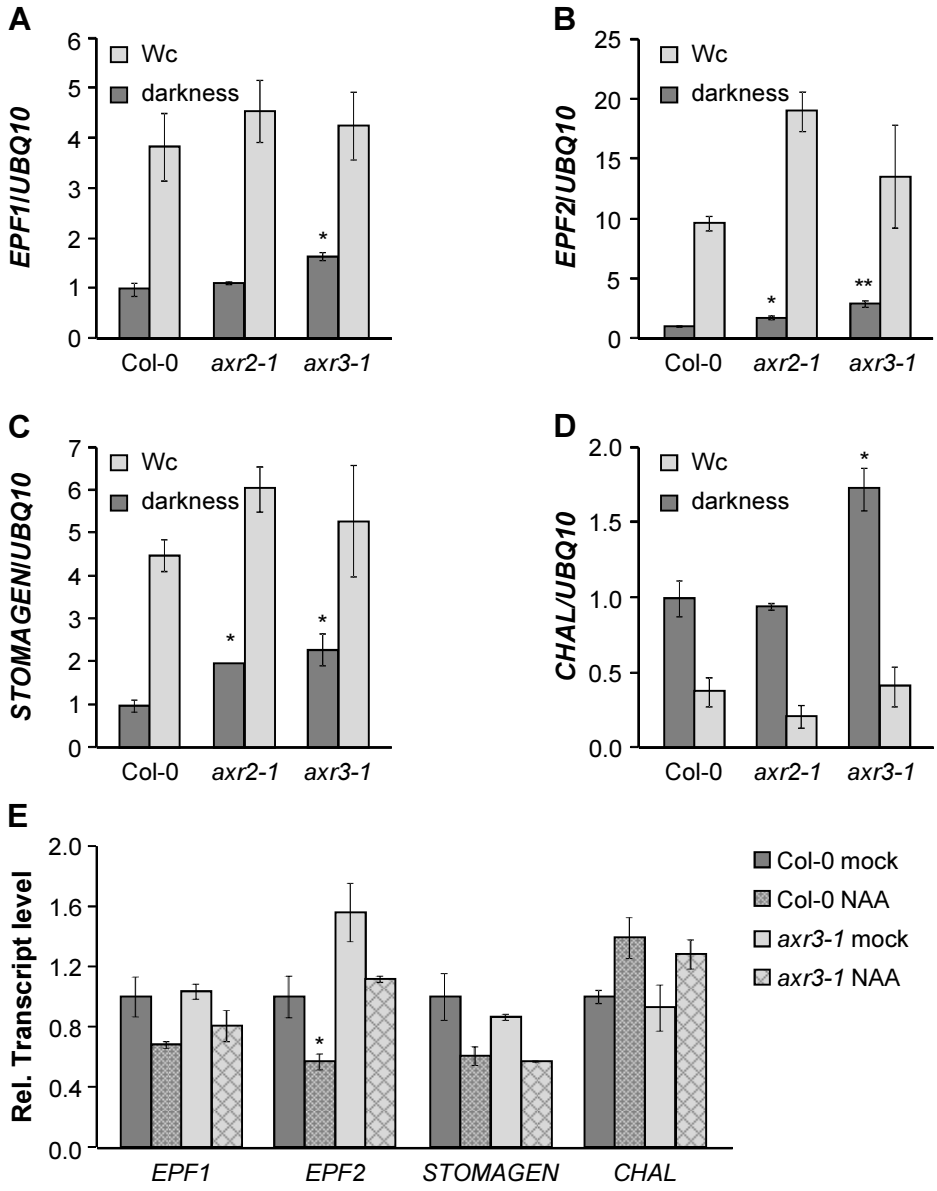

Fig. S9. Analysis of *EPFL* transcripts. (**A-D**) Transcript levels of *EPF1* (A), *EPF2* (B), *STOMAGEN* (C) and *CHAL* (D) in 5-d-old dark- or Wc-grown seedlings of the indicated genotypes. (**E**) *EPFL* transcript levels in 5-d-old Wc-grown Col-0 and *axr3-1* seedlings treated with 10 µM NAA or mock-treated. Transcript levels were normalised to *UBQ10* and are shown relative to the levels of dark-grown Col-0 seedlings (A-D) or the mock-treated Col-0 control (E). Error bars represent the s.e.m. Asterisks indicate significant differences to dark-grown wild type (A-D) or the mock-treated control (E) (*** $p < 0.001$, ** $p < 0.01$, * $p < 0.05$).

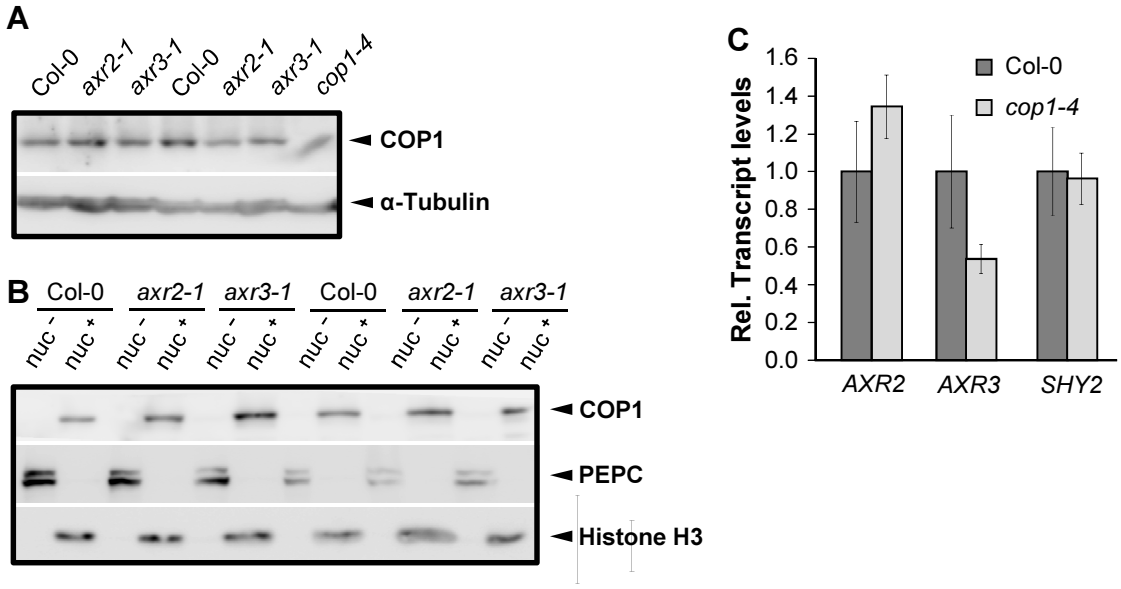

Fig. S10. Aux/IAA proteins and COP1 seem to act independently in light-dependent stomata development. (**A, B**) Immunodetection of COP1 protein in total protein extracts (A), nuclei-depleted (nuc^-) and nuclei-enrichted (nuc^+) protein fractions (B) of 5-d-old dark-grown Col-0, *axr2-1* and *axr3-1* seedlings. Tubulin is shown as loading control, PEPC is shown as cytosolic marker and histone H3 is shown as nuclear marker. The nuclei-enriched fractions were 15 x enriched compared to the nuclei-depleted fractions. Two independent biological replicates are shown. (**C**) Transcript levels of *AXR2*, *AXR3* and *SHY2* in 5-d-old dark-grown Col-0 and *cop1-4* seedlings. Transcript levels were normalised to *UBQ10* and are shown to relative to the levels of dark-grown Col-0 seedlings. Error bars represent the s.e.m.

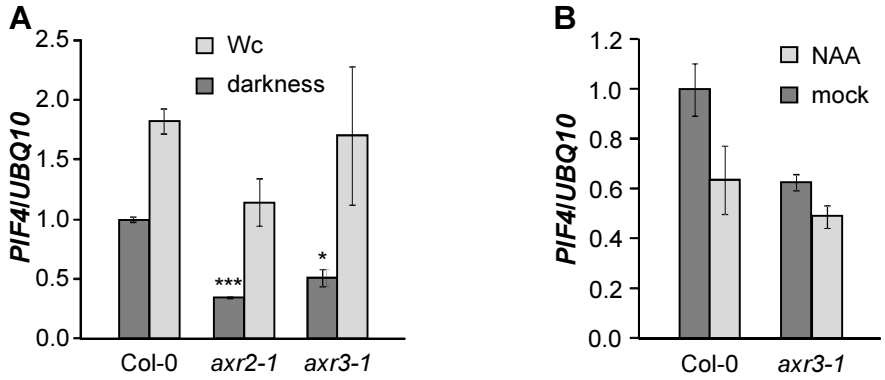

Fig. S11. Analysis of *PIF4* transcript. (**A**) Transcript levels of *PIF4* in 5-d-old dark- or Wc-grown seedlings of the indicated genotypes. (**B**) *PIF4* transcript levels in 5-d-old Wc-grown Col-0 and *axr3-1* seedlings treated with 10 µM NAA or mock-treated. Transcript levels were normalised to *UBQ10* and are shown relative to the levels of dark-grown Col-0 seedlings (A) or the mock-treated Col-0 control (B). Error bars represent the s.e.m. Asterisks indicate significant differences to dark-grown wild type (A) or the mock-treated control (B) (*** $p < 0.001$, ** $p < 0.01$, * $p < 0.05$).

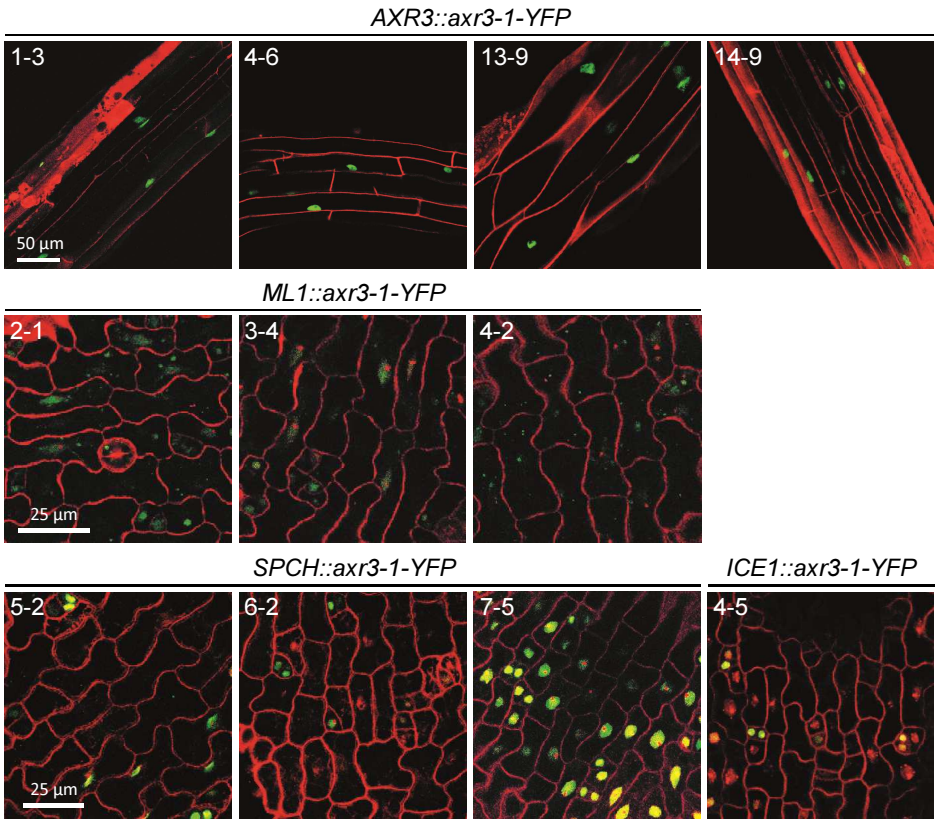

Fig. S12. Accumulation of axr3-1-YFP protein in dark-grown seedlings of additional *promoter::axr3-1-YFP* lines. Confocal images of the hypocotyl of Col-0 seedlings expressing axr3-1-YFP from the *AXR3* promoter (upper panel) and of the cotyledon epidermis of Col-0 seedlings expressing axr3-1-YFP from the *ML1* (middle panel), *SPCH* and *ICE1* (lower panel) promoters. Cell outlines were visualised by PI staining.

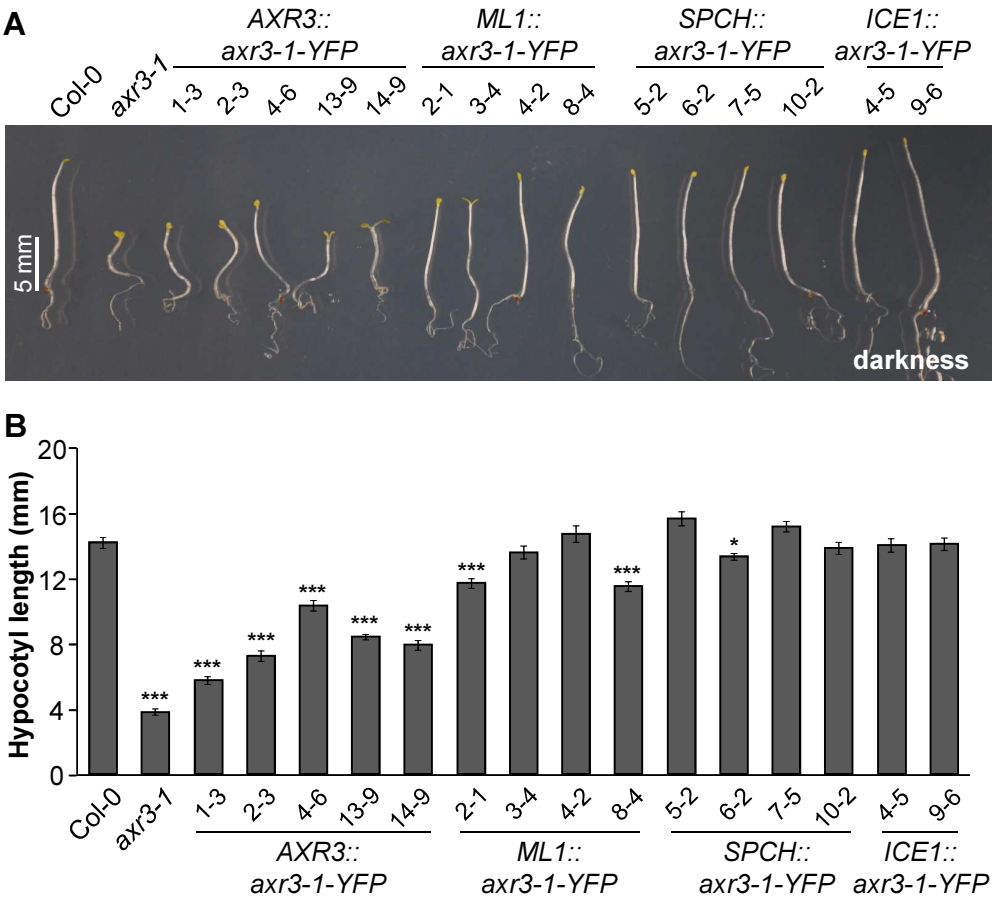

Fig. S13. Plants expressing axr3-1-YFP in the epidermis partially mimic the phenotype of dark-grown *axr3-1* seedlings. (**A**) Visual phenotype of 10-d-old dark-grown seedlings of the indicated *promoter::axr3-1-YFP* lines. Numbers denote independent transgenic lines. Dark-grown Col-0 and *axr3-1* seedlings are shown as controls. (**B**) Quantification of hypocotyl length of the lines shown in A. Error bars represent the s.e.m. Asterisks indicate significant differences in hypocotyl length compared to the wild type (*** $p < 0.001$, ** $p < 0.01$, * $p < 0.05$).

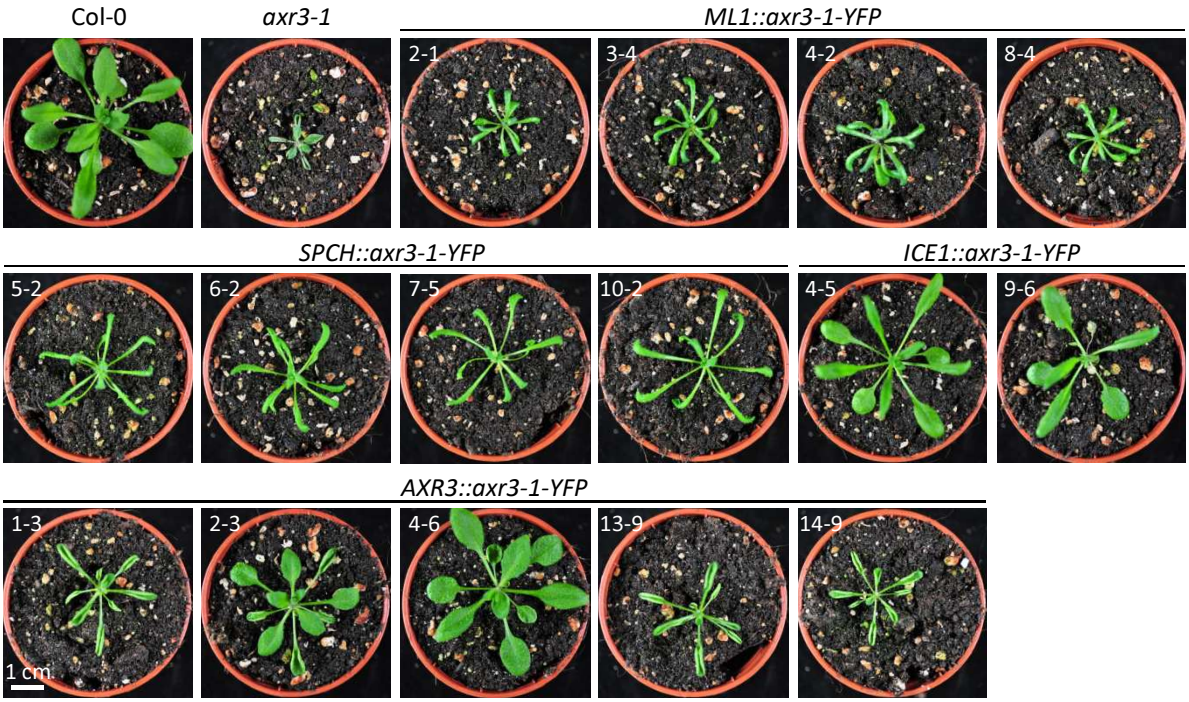

Fig. S14. The *axr3-1* adult plant phenotype is not completely mimicked by any *promoter::axr3-1-YFP* line. Visual phenotype of 24-d-old adult plants of the indicated *promoter::axr3-1-YFP* lines grown in long day conditions. Col-0 and *axr3-1* plants are shown as controls.

Supplementary Tables

Table S1. Primers and restriction enzymes used for genotyping.

Mutant	Primer name	Primer sequence	Restr. enzyme
axr2-1	AXR2-geno_F2	CAATACATACATGCGTACAAGC	MslI
	AXR2-geno_R2	ATGACTCTAACTCGGTAAGGTTC	
axr3-1	AXR3-geno_F1	TTTTCCACTCTTCTCTACTGCTC	BshTI
	AXR3-geno_R1	CTCCGTCCATTGATACCTTC	
cop1-4	COP1-geno_F1	GATGCGCTGAGTGGGCCA	HpyF10VI
	COP1-geno_R1	TGCCATTGTCCTTTTACCATTTCAGC	
er-105	ERg2248	AAGAAGTCATCTAAAGATGTGA	–
	Erg3016rc	AGAATTTTCAGGTTTGGAATCTGT	
	er-105	AGCTGACTATACCCGATACTGA	
erl1-2	ERL1-geno_F2	AGGGAAAAATACCAGTTGAGC	–
	ERL1-geno_R2	CGGAGAGATTGTTGAAGGAG	
	JL-202	CATTTTATAATAACGCTGCGGACA TCTAC	
erl2-1	ERL2-geno_F3	GAACTATCCCAGAGAGCATT	–
	ERL2-geno_R3	TGATTCAAGGCAGCACAG	
	JL-202	CATTTTATAATAACGCTGCGGACA TCTAC	
fama-1	FAMA-geno_F1	TGGTCTTGCTCGTTCTAGCTC	–
	FAMA-geno_R1	CTATCTTGCATGTCTTGCGTC	
	SALK-LBb1.3	ATTTTGCCGATTTCGGAAC	
mute-1	mute-dCAPS_F1	TTCGTTCTTTGACTCCTTGTTTCT ACCTCAAAAG	BslI
	mute-dCAPS_R1	CTTCGAGAAAATAATTAGGATTGT GAATTGAG	
spch-3	SPCH-geno_F1	GAAAAACCTAGATCCTCCCCC	–
	SPCH-geno_R3	AACCTGAAGAATCTCAAGAGCC	
	SAIL-LB1	GCCTTTTCAGAAATGGATAAATAG CCTTGCTTCC	
tmm-1	tmm-1-dCAPS_F1	AACGCGTTCAAAGGGCTCAAGAACGT	AclI
	tmm-1-dCAPS_R2	AGACTGTTATCGTTGAGCC	

Table S2. Primers used for qPCR.

Gene	Primer name	Primer sequence
AXR2	AXR2-RT_F2	AGAGTCCTGCCAAATCGG
	AXR2-RT_R2	TGAGATCAACGGTTTCGG
AXR3	AXR3-RT_F1	CTCTTTTACCATGGGCAAACATGGA
	AXR3-RT_R1	AGGGAACATAGTCCCAGCTATTCA
CHAL	CHAL-RT_F2	CATTACAACCATCAGAAAACACGAG
	CHAL-RT_R2	TGACACAGAGGACGAAGAAGAGTAG
EPF1	EPF1-RT_F2	GGCATTTACCAACATCCTCC
	EPF1-RT_R2	CCTCCTCCTCTGACGCTTC
EPF2	EPF2-RT_F2	CACTAAAAAACACGGTCAATGG
	EPF2-RT_R2	TGCTTATTTCCTTCTTGTGGTG
ER	ER-RT_F2	GACTCTTGATTGGGACACACG
	ER-RT_R2	AGAATGTTGGACGACTTCACG
ERL1	ERL1-RT_F1	GCAGCAAGAGAATGAAGTTAGG
	ERL1-RT_R1	AACCATCCTTTCCTTCCAATC
ERL2	ERL2-RT_F2	AAGTGATTTAGGGCTAGTATGAGGG
	ERL2-RT_R2	GAACTCGTGAAGATGTCCATTG
FAMA	FAMA-RT_F2	CTGCTTTGGAGGATCTTCATCTCT
	FAMA-RT_R2	CTTCTGCCGTAAACCTCGTTTC
MUTE	MUTE-RT_F2	GACGATCACTTCATCAGACACAAAG
	MUTE-RT_R2	CCTCAATATTAGTAGCATGGAGGAGACT
PIF4	PIF4-RT_F1	GCTTCGGCTCCGATGAT
	PIF4-RT_R1	CGCGGCCTGCATGTGTG
SHY2	SHY2-RT_F1	CTTAAAGCTTTAGAAGTGATGTTCAA
	SHY2-RT_R1	CACGTACATATGAACATCTCCCA
SPCH	SPCH-RT_F2	TTCTGCACTTAGTTGGCACTCAAT
	SPCH-RT_R2	GCTGCTCTTGAAGATTTGGCTCT
STOMAGEN	STOM-RT_F2	AATACGGTCTCCCTTCTCCC
	STOM-RT_R2	CTGGAACTTGCTCTGCTCTG
TMM	TMM-RT_F3	AACAGTCTTCGGGTCCTTCAC
	TMM-RT_R3	GCTCGCTTAGATGCTTCACG
UBQ10	UBQ10-RT_F	CACACTCCACTTGGTCTTGCGT
	UBQ10-RT_R	TGGTCTTTCCGGTGAGAGTCTTCA

Table S3. Primers used for cloning.

Primer name	Primer sequence
AXR3pro-attB-F	GGGGACAAGTTTGTACAAAAAAGCAGGCTTGTGGTAGAATGTTGAGAGTTGTGGC
AXR3pro-attB-R	GGGGACCACTTTGTACAAGAAAGCTGGGTTATTAACCTTTCTTCTTCTTTGGTGTTC
AXR3-XhoI-R	CATGCTCGAGAGCTCTGCTCTTGCACTTCTCC
HindIII-AXR3-F	CTTGAAGCTTATGATGGGCAGTGTCGAGCTG
ICE1pro-attB-F	GGGGACAAGTTTGTACAAAAAAGCAGGCTACCGGACCACCGTCAATAACATCG
ICE1pro-attB-R	GGGGACCACTTTGTACAAGAAAGCTGGGTCGCCAAAGTTGACACCTTTACCC
SPCHpro-attB-F	GGGGACAAGTTTGTACAAAAAAGCAGGCTCAAGATCATCACTGCGATAAGGAG
SPCHpro-attB-R	GGGGACCACTTTGTACAAGAAAGCTGGGTCGTGATTAGAGATATATCCTTCTC
XhoI-YFP-F	GCATCTCGAGATGGTGAGCAAGGGCGAGGAG
YFP-SpeI-R	TCACACTAGTCTACTTGTACAGCTCGTCCATGC